

<sup>1</sup> **High-resolution regional climate model evaluation using variable-resolution**

<sup>2</sup> **CESM over California**

<sup>3</sup> Xingying Huang, \* Alan M. Rhoades and Paul A. Ullrich

<sup>4</sup> *Department of Land, Air and Water Resources, University of California, Davis*

<sup>5</sup> Colin M. Zarzycki

<sup>6</sup> *National Center for Atmospheric Research*

<sup>7</sup> \*Corresponding author address: Xingying Huang, Department of Land, Air and Water Resources,

<sup>8</sup> University of California Davis, Davis, CA 95616.

<sup>9</sup> E-mail: xyhuang@ucdavis.edu

## ABSTRACT

10

<sup>11</sup> **1. Introduction**

<sup>12</sup> Global climate models (GCMs) have been widely used to simulate both past and future cli-  
<sup>13</sup> mate. Although GCMs have been demonstrated to successfully represent large-scale features of  
<sup>14</sup> the climate system, they are usually employed at coarse resolutions ( $\sim 1$  degree), largely due to  
<sup>15</sup> computational limitations. Global climate reanalysis datasets, which assimilate climate obser-  
<sup>16</sup>vations using a climate model, can represent a best estimate of historical weather patterns, but  
<sup>17</sup> still have relatively low resolutions no finer than  $0.5^\circ$  (<http://reanalyses.org/atmosphere/overview-current-reanalyses>). Consequently, regional climate is not well captured by either GCMs or global  
<sup>18</sup> reanalysis datasets. However, dynamical processes at unrepresented scales are significantly drivers  
<sup>19</sup> for regional and local climate variability, especially over complex terrain (Soares et al. 2012). In  
<sup>20</sup> order to capture these fine-scale dynamical features, high horizontal resolution is needed to allow  
<sup>21</sup> a more accurate representation of fine scale forcing, processes and interactions (see, for example,  
<sup>22</sup> Leung et al. (2003); Rauscher et al. (2010)). We anticipate a better representation of regional cli-  
<sup>23</sup>mate information can better inform local stakeholders and policymakers towards action on climate  
<sup>24</sup> change and mitigation.

<sup>26</sup> In order to model regional climate at high spatial and temporal resolution over a limited area,  
<sup>27</sup> downscaling methods have been developed. There are largely two approaches for downscaling:  
<sup>28</sup> The first is statistical downscaling, which aims to estimate fine scale behavior via analysis of the  
<sup>29</sup> relationships between observed variables at different scales (Fowler et al. 2007). This method is  
<sup>30</sup> empirical and cannot be used if the observed relationships do not hold with a changing climate  
<sup>31</sup> (Soares et al. 2012). The second approach is dynamical downscaling, which uses a numerical  
<sup>32</sup> model to simulate higher spatial resolution conditions in greater detail. Dynamical downscaling  
<sup>33</sup> is popular and commonly employed, using nested limited-area models (LAMs) to model regional

<sup>34</sup> scales (Laprise et al. 2008). In this context, LAMs are typically referred as regional climate models  
<sup>35</sup> (RCMs) when applying to climate scales. RCMs are forced by output of GCMs or reanalysis data,  
<sup>36</sup> and have been widely used, particularly to capture physically consistent regional and local circu-  
<sup>37</sup> lations at the needed spatial and time scales (Christensen et al. 2007; Bukovsky and Karoly 2009;  
<sup>38</sup> Caldwell et al. 2009; Mearns et al. 2012). More recently, variable-resolution global climate models  
<sup>39</sup> (VRGCMs) have been more widely employed for modeling regional climate. This approach uses  
<sup>40</sup> a global model that includes high-resolution over a specific region and lower resolution over the  
<sup>41</sup> remainder of the globe (Staniforth and Mitchell 1978; Fox-Rabinovitz et al. 1997). VRGCMs have  
<sup>42</sup> been demonstrated to be effective for regional climate studies and applications, owing to the ad-  
<sup>43</sup> vantages of traditional GCMs in representing large-scale features, at a reduced computational cost  
<sup>44</sup> compared to uniform GCMs (Fox-Rabinovitz et al. 2001, 2006; Rauscher et al. 2013; Zarzycki  
<sup>45</sup> et al. 2014; Zarzycki and Jablonowski 2014; Zarzycki et al. 2015a).

<sup>46</sup> Compared with RCMs, a key advantage of VRGCMs is the use a single, unified modeling frame-  
<sup>47</sup> work, rather than a separate GCM and RCM. Thus VRGCMs avoid potential inconsistency be-  
<sup>48</sup> tween the global and regional domains, and naturally support two-way interaction between these  
<sup>49</sup> domains without the need for nudging (Warner et al. 1997; McDonald 2003; Laprise et al. 2008;  
<sup>50</sup> Mesinger and Veljovic 2013). However, in order to obtain deeper insight into the performance  
<sup>51</sup> of these two modeling approaches, it is necessary to compare them directly. For the purposes of  
<sup>52</sup> this paper, we will focus on the recently developed variable-resolution Community Earth System  
<sup>53</sup> Model (varres-CESM) as our VRGCM of interest. CESM is a state-of-the-art Earth modeling  
<sup>54</sup> framework developed at NCAR, consisting of atmospheric, oceanic, land and sea ice compo-  
<sup>55</sup> nents (Neale et al. 2010). Although CESM has been well-used for uniform resolution modeling,  
<sup>56</sup> variable-resolution in the Community Atmosphere Models (CAM) Spectral Element (SE) dynam-  
<sup>57</sup> ical core has only been recently developed and has never be investigated for long-term regional

climate simulation (Taylor and Fournier 2010; Zarzycki et al. 2014). Consequently, the goal of this paper is to evaluate the performance of varres-CESM against gridded observational data, reanalysis data and as compared to a dynamically downscaled modeling strategy. Our variable-resolution simulations will focus on relatively high resolutions for climate assessment, namely 28km and 14km regional resolution, which are much more typical for dynamically downscaled studies. For comparison with dynamical downscaling, the Weather Research and Forecasting (WRF) model will be used (Skamarock et al. 2005). WRF has gained wide acceptance to study regional climate over the past decade, showing its adequate capability in representation of mean fine-scale climate properties (Lo et al. 2008; Leung and Qian 2009; Soares et al. 2012). We anticipate that this assessment will add value in modeling mean regional climatology and improve our understanding about the effects of multi-scale processes in regional climate regulation. Our goal is also to advance the better use of models in future climate predictions and climatic extremes studies regionally.

Simulations using both varres-CESM and WRF have been performed for 26 years of historical climate with a regional domain centered on the state of California (CA). With its complex topography, coastal influences, and wide latitudinal range, this makes CA an excellent test bed for high-resolution climate studies. Also, an understanding of local climate variability is incredibly important for policymakers and stakeholders in California due to its vast agricultural industry, wide demographics, and vulnerability to anthropogenically-induced climate change (Hayhoe et al. 2004; Cayan et al. 2008). RCM simulations over California have also been conducted in previous studies (Leung et al. 2004; Kanamitsu and Kanamaru 2007; Caldwell et al. 2009; Pan et al. 2011; Pierce et al. 2013). Caldwell et al. (2009), in particular, presented results from WRF (Weather Research and Forecasting) at 12km spatial resolution showing both the overall consistency and certain bias between simulations and observations (Caldwell et al. 2009). The paper is organized as follows. Section 2 describes the model set up, evaluation methods and verification data. In

82 Section 3, results are demonstrated focusing on 2 m temperature (Ts) and precipitation (Pr). Key  
83 results are summarized and further discussion is made in section 4.

84 **2. Models and Methodology**

85 *a. Simulation design*

86 All simulations use the AMIP (Atmospheric Model Intercomparison Project) protocols with  
87 prescribed sea-surface temperatures. The ocean model is disabled.

88 1) WRF

89 The fully compressible non-hydrostatic WRF-ARW model, version 3.5.1 is used. ERA-Interim  
90 pressure-level reanalysis was used to provide initial, lateral conditions and sea surface tempera-  
91 tures (SST) for the domains every 6 hours. ERA-Interim reanalysis ( $\sim 80$  km) has been widely  
92 used and validated for its reliability as forcing data (Dee et al. 2011). Two simulations are con-  
93 ducted with a maximum horizontal resolution of 27km (WRF27) and 9km (WRF9) respectively,  
94 over the time period 1979-01-01 to 2005-12-31 (UTC). The  $\sim 10$  km resolutions are actually finer  
95 than most former studies for long-term climate.

96 The simulation domains of WRF9 are depicted in Figure 1. For the WRF27 simulation, one do-  
97 main (same as the outer domain of WRF9) is used. For the WRF9 simulation, two nested domains  
98 are used with outer domain at 27km (same as the WRF27) and inner domain at 9km horizontal  
99 grid resolution, with two-way nesting enabled. These choices have been made to satisfy the natu-  
100 ral WRF aspect ratio of 3:1. Both grids are centered on CA and have respectively,  $120 \times 110$  and  
101  $151 \times 172$  grid points. Around the boundaries 10 grid points are used as lateral relaxation zones.  
102 Since simulations cover climatological time scales, SSTs are updated each 6 hours. In order to  
103 reduce the drift between forcing data and RCM, grid nudging (Stauffer and Seaman 1990) was

104 applied to the outer domain every 6 hours at all levels except the planetary boundary layer (PBL)  
105 as suggested by Lo et al. (2008). This setup uses 41 vertical levels with top pressure at 50 hPa.  
106 We use the following parameterization options for the standard settings: WSM 6-class graupel  
107 microphysics scheme (Hong and Lim 2006), Kain-Fritsch cumulus scheme (Kain 2004), CAM  
108 shortwave and longwave radiation schemes (Collins et al. 2004) (??). These settings are supported  
109 by the one-year test running result with different options. Also, the Yonsei University (YSU)  
110 boundary layer scheme (Hong et al. 2006), and Noah Land Surface Model (Chen and Dudhia  
111 2001) are chosen as commonly used for climate applications considering long-term reliability and  
112 computational cost.

## 113 2) VARRES-CESM

114 CESM has been under development for nearly two decades, and has been used heavily in better  
115 understanding the effects of global climate change (Hurrell et al. 2013). Here, CAM version 5  
116 (CAM5) and the Community Land Model (CLM) version 4 are used. As mentioned earlier, SE is  
117 currently the default dynamical core in CAM along with recently added variable-resolution grid  
118 support. For our study, the variable-resolution cubed-sphere grids are generated within both CAM  
119 and CLM with the open-source software package SQuadGen (Ullrich 2014). The grids used are  
120 depicted in Figure 2. These grids correspond to 0.25 degree ( $\sim 28\text{km}$ ) and 0.125 degree ( $\sim 14\text{km}$ )  
121 maximum horizontal resolution, with 1 degree resolution away from the regional domain. These  
122 resolutions have been selected since CAM-SE naturally supports a 2:1 aspect ratio, meaning there  
123 are two transition layers from 1 degree to 0.25 degree, and one additional transition from 0.25  
124 degree to 0.125 degree. As with the WRF simulations, the time period from 1979-01-01 to 2005-  
125 12-31 (UTC). Corresponding fine-scale topography files have been produced similarly as Zarzycki  
126 et al. (2015b). Land surface data at 50 km resolution is used. Tuning parameters are not modified

127 from their default configuration. Greenhouse gas (GHG) concentrations are prescribed based on  
128 historical observations. SSTs and ice coverage are supplied by the 1degree Hadley Centre Sea Ice  
129 and Sea Surface Temperature dataset (HadISST) (Hurrell et al. 2008).

130 **Detailed settings for varres-CESM (to be added)**

131 *b. Datasets*

132 Our evaluation focuses on near surface air temperature and precipitation, representative of the  
133 mean regional climate and climate variability on monthly, season and annual time scales. Re-  
134 analysis and gridded observational datasets of the highest quality available (described in Table 1)  
135 are employed as reference. These data products incorporate station measurements, satellite in-  
136 formation and other observational data. Although these products are generally based on similar  
137 measurements, they are scaled and gridded using different techniques, causing processing uncer-  
138 tainty except of measurement error. Variation between reference products represents observational  
139 uncertainty. We acknowledge that reanalysis products are particularly sensitive to model choice  
140 and choice of assimilated observations and so cannot be treated as truth. Our assessment focuses  
141 on the performance of the WRF and CESM simulations in terms of both mean behavior and vari-  
142 ability.

143 (i) *NARR*: The North American Regional Reanalysis (NARR) (Mesinger et al. 2006) provides  
144 dynamically downscaled data over North America at  $\sim 32$  km resolution and 3 hourly intervals  
145 from 1979 through present. All major climatological variables are present in NARR, making it  
146 an excellent candidate for assessment of regional extremes. Nonetheless, some inaccuracies have  
147 been identified in NARR that must be accounted for, including deficiencies in precipitation fields  
148 away from the continental US (Bukovsky and Karoly 2007).

149 (ii) *Daymet*: Daymet is an extremely high resolution (1 km) gridded dataset with daily outputs  
150 covering the period of 1980 through 2013 and including total precipitation, humidity and mini-  
151 mum and maximum temperatures (Thornton et al. 1997; Thornton and Running 1999; Thornton  
152 et al. 2000). The dataset is produced using an algorithmic technique that ingests point station  
153 measurements in conjunction with a truncated Gaussian weighting filter. Some adjustments are  
154 made to account for topography. Daymet is available through the Oak Ridge National Laboratory  
155 Distributed Active Archive Center (ORNL DAAC).

156 (iii) *PRISM*: The Parameter-elevation Regressions on Independent Slopes Model (PRISM)  
157 (Daly et al. 2008) supports a 4km gridded dataset obtained by taking point measurements and  
158 applying a weighted regression scheme that accounts for many factors affecting the local cli-  
159 matology. The datasets include total precipitation and minimum, maximum and (derived) mean  
160 temperatures. Monthly climatological variables are available for 1895 through 2014. Daily data is  
161 available for the period 1981 through present, although the documentation is careful to state that  
162 since the observational input changes over time this data is not intended for multi-decadal trends.  
163 This dataset will be used for detection and characterization of temperature and precipitation ex-  
164 tremes.

165 (iv) *UW*: The UW daily gridded meteorological data is obtained from the Surface Water Mod-  
166eling group at the University of Washington (Maurer et al. 2002; Hamlet and Lettenmaier 2005).  
167 UW made topography correction through forcing the long-term average precipitation to match that  
168 of PRISM dataset. Ts dataset is produced similarly to precipitation, but used a simple 6.1 K/km  
169 lapse rate for topographic effect instead of forcing to match towards PRISM.

170 Also, output from globally uniform CESM with 25km spatial resolution is compared together to  
171 see if variable-resolution CESM perform similarly or even better in modeling mean climatology.

<sup>172</sup> This globally uniform simulation used an earlier version of CAM, CAM5-FV (finite volume). And  
<sup>173</sup> this dataset is described in additional detail in Wehner et al. (2014a) and Wehner et al. (2014b).  
<sup>174</sup> Note that the appendix of the latter paper lists parameters that are different from the public release.

<sup>175</sup> *c. Post-processing*

<sup>176</sup> For sake of consistency, reference data are averaged to models' output resolution only when  
<sup>177</sup> showing the differences or calculating related statistical values (e.g. root mean square error  
<sup>178</sup> (RMSE), bias, and correlation). Bilinear interpolation method is used for regular 2D grid. Bi-  
<sup>179</sup> linear interpolation is probably not the best technique; when the reference data is higher resolution  
<sup>180</sup> than the model output you should average to a model grid cell. When the reference data is coarser  
<sup>181</sup> resolution, it is usually not desirable to interpolate to a finer grid – this does not take into account  
<sup>182</sup> topographic features which can greatly affect the results.

<sup>183</sup> In order to get in-depth analysis of California's varied climate regions, here we divide the state  
<sup>184</sup> into 5 regional zones, including central valley, mountain region, North coast, South coast and  
<sup>185</sup> desert, as Figure 1 shows. Simulations and datasets are masked to get climate features in each  
<sup>186</sup> region. First year of simulations was treated as model spin-up, thus, all the data analysis are based  
<sup>187</sup> on the period from 1980 to 2005, i.e. 26 years.

<sup>188</sup> **3. Results**

<sup>189</sup> The grid-scale topography for the different simulations are contrasted in Figure 3. The higher  
<sup>190</sup> resolution models provide a clearly improved representation of local topography. This is impor-  
<sup>191</sup> tant for understanding climate simulations since topography is an important driver for fine-scale  
<sup>192</sup> dynamic processes, especially over complex terrain. Some differences are also apparent between  
<sup>193</sup> the 28km varres-CESM and 27km WRF model, particularly over the central valley, and indicative

194 of different methodology for preparation of the topography dataset. In this section, we assess the  
195 models' performance in terms of both temperature and precipitation. In particular, our comparison  
196 will focus on daily maximum, minimum and average 2m temperatures (Tmax, Tmin and Tavg),  
197 and daily precipitation (Pr) both annually and seasonally. These variables are the most relevant for  
198 a base-line climate assessment.

199 *a. Computational Cost*

200 The running time for a daily file is about 6 minutes and 26 minutes for varres-CESM 28km and  
201 varres-CESM 14km respectively, with 2 minutes and 25 minutes for WRF 27km and WRF 9km  
202 respectively. **for uniform CESM ??**

203 *b. Temperature*

204 Here, Tmax, Tmin and Tavg from varres-CESM, WRF and reference datasets over the simula-  
205 tion period are analyzed based on daily averaged results. We focused on the summer and winter  
206 seasons, i.e. June-July-August (JJA) and December-January-February (DJF).

207 The JJA Tmax and Tmin climatology are shown in Figures 4, 5. For Tmax, generally, simu-  
208 lations show similar regional patterns to observations, but with a warmer central valley. varres-  
209 CESM also showed positive bias over mountain region, especially for coarser simulation. On the  
210 contrary, WRF displayed cold bias over other regions, particular for finer-scale simulation. For  
211 Tmin, varres-CESM showed larger bias than Tmax, with obvious warmer bias over most regions.  
212 WRF seems to better simulate Tmin than varres-CESM with smaller bias, with both warm and  
213 cold bias over individual climate zones. However, errors are relatively smaller when comparing  
214 with PRISM than with UW, so, uncertainty among different observations must also be considered  
215 here. Tavg is also showed in part of Figure 6. varres-CESM still exhibited warm bias, and WRF

216 showed smaller bias. The RMSE for these models are basically ranges from 1 to 3 K, as showed  
217 by Table 2. RMSE and bias are calculated based on the 26-year average value of models and  
218 reference dataset over California. Overall, varres-CESM 0.125 deg performs best for long-term  
219 Tmax simulation, and WRF9 has largest error. And WRF is better at modeling Tmin than varres-  
220 CESM. There are about +2 K SST bias near the coast between varres-CESM and WRF. This may  
221 explain part of the reason. In this way, varres-CESM overestimated JJA climatology especially  
222 for Tmin, however, WRF underestimated Tmax and Tavg. Comparing with NARR, the biases for  
223 JJA Tmin and Tavg modeling largely reduced for varres-CESM. This means that in this respect,  
224 varres-CESM results are similarly as other GCMs output assimilated in NARR.

225 Although California is known for warm climate, the DJF climatology is still discussed here for  
226 relatively complete analysis. For Tmax (Figure 7), all simulations showed warm bias at central  
227 valley especially for WRF27 but cold bias over almost all other regions particularly for WRF9.  
228 For Tmin (Figure 8), models showed warm bias over most regions except partly highest mountain  
229 region, and errors are smaller when comparing with PRISM than with UW. For Tavg (part Figure  
230 6), biases are quite smaller between models and PRISM dataset. Overall, the RMSEs are still  
231 controlled between 1 and 3 K, as showed by Table 3. Simulations at coarser resolution seem  
232 perform better, especially for varres-CESM 0.25deg in Tmax, however, varres-CESM 0.25deg  
233 showed largest error in modeling Tmin.

234 For both JJA and DJF climatology, nevertheless, correlations are high between simulations and  
235 observations (>0.95), especially for Tmax and Tavg, and the error is relative acceptable overall.  
236 Not surprisingly, NARR shows obvious differences from other gridded observations, however,  
237 uncertainty between observational datasets are much smaller than the models' biases, unlikely  
238 impacting our results. Also, appearance of sea breeze can be observed in varres-CESM runs.

239 The seasonal cycle of Tavg is showed in Figure 9. The standard deviation values are computed  
240 from the 26 yearly average values for each month. Models do show good consistency with ref-  
241 erence data with about no larger than 2 K bias, mainly in coldest and hottest seasons. However,  
242 varres-CESM do show smaller bias than WRF at summer season except over mountain region, and  
243 WRF did better at winter season. Varres-CESM seems to be colder in winter and WRF is not hot  
244 enough in summer. And varres-CESM showed larger variability among seasons than observations,  
245 while WRF shows opposite trend. No obvious divergence can be detected between multi-scales,  
246 though coarser simulations even result a littler better than finer ones. Also, seasonal trends are  
247 similar among sub-zones, though showing diverse magnitudes, and models seem to perform less  
248 better over coastal region. As for the multi-year monthly variability, models are quite close to  
249 reference dataset around 4 K, except in winter season, especially at January, varres-CESM and  
250 WRF 9km show about half time and one time larger values respectively.

251 For the temperature climatology in California, we are more interested in the summer season,  
252 especially the Tmax value due to the hot summer. Here, we depicted the frequency distribution of  
253 Tmax constructed from 26 years summer daily data in Figure 10. Similar distribution shapes are  
254 showed by both models and observations, though biases are noticed between them (even within  
255 observations). Models are more consistent with observations over upper bound than lower bound.  
256 For hot events detection, both varres-CESM and WRF27 exhibit satisfactory performance over  
257 most regions except in central valley (CV). No obvious improvement is showed by higher reso-  
258 lution in varres-CESM. Models show obviously larger upper tail than observations in CV. As we  
259 already showed above, models do overestimate Tmax annually in CV. In order to further check  
260 the accuracy of the gridded observations, we examined the Tmax data from the weather stations  
261 distributed over the CV. The results show that it is true that Tmax above 45C are rarely recorded.  
262 The reasons of the large bias for extreme hot days modeling can be manifold showed in both

263 varres-CESM and WRF over CV. Caldwell et al. (2009) stated that this bias pattern is consistent  
264 with overly dry summertime soil moisture. This can be caused by insufficient physical parame-  
265 terization and the lack of accurate land surface treatment in climate models. Other reasons may  
266 include the limited observations and unevenly distributed stations for gridded datasets. **table of**  
267 **first four moments or just describe directly?**

268 *c. Precipitation*

269 Since the precipitation is mainly from winter season in California, here, the annual and DJF  
270 precipitation are described.

271 The long-term annual average climatology of daily precipitation (Pr) from varres-CESM, WRF  
272 and reference dataset are displayed by Figure 11. Comparing with observations, simulations do  
273 capture regional patterns of precipitation. Precipitation distributes mostly along the north coastal  
274 part and Sierra mountains, and relatively low over other regions. However, there exist obvious dif-  
275 ferences among simulations. varres-CESM overestimate a little especially for coarser simulation at  
276 the western side of Sierras, and finer simulation has reduced that bias showing the improvementnt  
277 of orographic effects. Notably, large difference showed between WRF27 and WRF9. WRF27  
278 underestimated a little, but WRF9 greatly showed obvious positive absolute error at North coastal  
279 part and the Sierra where maximum precipitation is distributed, and the relative bias can reach 50  
280 percent. Overall, models perform satisfactorily except for WRF9, and varres-CESM 0.125d per-  
281 form a little better than CESM 0.25d and WRF27, as further showed by the RMSE and bias value  
282 in Table 4. Observations also demonstrate noticeable differences indicating uncertainty inherent  
283 in interpolating station data to a grid. However, these observations are still of the highest quality  
284 available and the uncertainty is relatively small comparing the simulations, and our conclusions  
285 can hold.

286 The DJF precipitation from models and reference data as plotted in Figure 12. We can see that  
287 models and reference data show similar pattern as annual, though the precipitations almost doubles  
288 in winter comparing with annual value. varres-CESM still overestimate with larger absolute bias,  
289 especially at central valley ([possible reasons ???](#)), and higher resolution still performs better. WRF  
290 27km underestimate a little, and WRF 9km still greatly overestimate at North coastal region and  
291 the sierra region. Considering the relatively heavy winter precipitation, the relative error is still  
292 acceptable for varres-CESM and WRF 27km, with RMSE and bias values showed in Table 4.

293 The climatological annual cycle of precipitation averaged over each sub regions is presented in  
294 Figure 13. It can be seen that bias mainly occurred during rainy seasons especially in winter. WRF  
295 27km is dryer, and varres-CESM is wetter especially in winter season. WRF 9km is too wetter as  
296 found already and showed obviously larger variability than observations. varres-CESM showed a  
297 little larger variability among rainy seasons than observations, while WRF 27km shows opposite  
298 trend. The seasonal trend proves what we know about the strong seasonality of California Pr with  
299 high values in the winter and almost no precipitation during the summer. Overall, varres-CESM  
300 are better consistent with observations at most regions in all seasons comparing with WRF, as  
301 showed in Table 5. [add the plot of 26 years precipitation time trend?](#)

302 Further, the frequency distribution of winter Pr constructed from 26 years rainy days  
303 ( $Pr_i=0.1\text{mm/d}$ ) is depicted in Figure 14. It can be seen that varres-CESM is more consistent with  
304 observations except at Central Valley, where WRF 27km performs much better as former figures  
305 already showed. varres-CESM 0.25d and varres-CESM 0.125d do not show meaningful differ-  
306 ences. However, WRF 27km shows underprediction of rainy days, especially for moderately rainy  
307 events, and, not surprisingly, WRF 9km obviously over-prediction rainy days particular when rain-  
308 ing goes stronger. For strong precipitation events, varres-CESM and WRF 27 shows satisfactory  
309 modeling ability over most regions except at Central Valley for varres-CESM, though observa-

310 tions also show uncertainties. We also notice the drift of the peak value between the varres-CESM  
311 and observations or even with the two varres-CESM runs due to the internal model variability of  
312 CESM. As a GCM, varres-CESM is not forced by reanalysis dataset like WRF, therefore, it is not  
313 surprising that time drift occurred when dealing with seasonal trend.

314 The positive bias of precipitation using WRF at high resolution has also been found in former  
315 studies. Caldwell et al. (2009) gave a detailed discuss of the possible reasons, stating that bias  
316 comes from a variety of source like the model itself and partly the physics schemes. And this  
317 is out of the scope of this paper, further discussion can be found in former studies (Jankov et al.  
318 2005; Gallus Jr and Bresch 2006; Chin et al. 2010; Caldwell 2010).

319 At last, a concise summary of model performance annually over CA is provided by the Taylor  
320 diagram (Figure ??). This diagram includes the spatial correlation between the simulated and ob-  
321 served fields, the RMS variability of simulations normalized by that in the observations, and mean  
322 biases from verification data symbolized at (1,0). It can be seen that models are close to reference  
323 data (PRISM), with small biases for temperature variables. Normalized standard deviation and  
324 bias are larger for precipitation, especially for WRF 9km. varres-CESM performed better than  
325 WRF generally with opposite bias value in some cases. Overall, varres-CESM showed its compa-  
326 rable ability in studying high-resolution regional climatology against with regional climate model  
327 WRF.

328 *d. varres-CESM and uniform CESM*

329 The climatology simulations of both varres-CESM 0.25 deg and uniform CESM-FV 0.25 deg  
330 are showed in Figure 16 including Tmax, Tmin, Tavg and Pr. For JJA temperature, these two  
331 simulations show similar results. Differences are displayed in DJF temperature, uniform CESM  
332 showed smaller values than varres-CESM, which resulted less bias over central valley but larger

333 bias over most other regions. For annual precipitation, comparing with varres-CESM, uniform  
334 CESM has obviously less bias over central valley. However, uniform CESM overestimated over  
335 part of northern coast and mountain regions in DJF Pr. In sum, Ccomparing with the uniform  
336 resolution CESM-FV simulation, varres-CESM performed similarly or even better in some cases.  
337 This will add the value to the use of variable-resolution GCMs for assessing climate change over  
338 the coming century.

#### 339 **4. Discussions and summary**

340 This study evaluated the performances of varres-CESM against WRF which is a dynamically  
341 downscaled modeling strategy with gridded reference datasets. As the need of regional climate  
342 studies is increasing, this study explored the use of both a variable-resolution global climate model  
343 and a traditional regional climate model to improve our understanding of the effects of fine-scale  
344 processes in regional climate regulation. Based on the 26 years of historical climate simulation  
345 centered on California, we found that

346 *Acknowledgments.*

#### 347 **References**

- 348 Bukovsky, M. S., and D. J. Karoly, 2007: A brief evaluation of precipitation from the North  
349 American Regional Reanalysis. *Journal of Hydrometeorology*, **8** (4), 837–846.
- 350 Bukovsky, M. S., and D. J. Karoly, 2009: Precipitation simulations using WRF as a nested regional  
351 climate model. *Journal of Applied Meteorology and Climatology*, **48** (10), 2152–2159.
- 352 Caldwell, P., 2010: California wintertime precipitation bias in regional and global climate models.  
353 *Journal of Applied Meteorology and Climatology*, **49** (10), 2147–2158.

- 354 Caldwell, P., H.-N. S. Chin, D. C. Bader, and G. Bala, 2009: Evaluation of a WRF dynamical  
355 downscaling simulation over California. *Climatic Change*, **95** (3-4), 499–521.
- 356 Cayan, D. R., A. L. Luers, G. Franco, M. Hanemann, B. Croes, and E. Vine, 2008: Overview of  
357 the California climate change scenarios project. *Climatic Change*, **87** (1), 1–6.
- 358 Chen, F., and J. Dudhia, 2001: Coupling an advanced land surface-hydrology model with the Penn  
359 State-NCAR MM5 modeling system. Part I: Model implementation and sensitivity. *Monthly*  
360 *Weather Review*, **129** (4), 569–585.
- 361 Chin, H.-N. S., P. M. Caldwell, and D. C. Bader, 2010: Preliminary study of California wintertime  
362 model wet bias. *Monthly Weather Review*, **138** (9), 3556–3571.
- 363 Christensen, J. H., and Coauthors, 2007: Regional climate projections. *Climate Change, 2007:*  
364 *The Physical Science Basis. Contribution of Working group I to the Fourth Assessment Report*  
365 *of the Intergovernmental Panel on Climate Change, University Press, Cambridge, Chapter 11,*  
366 847–940.
- 367 Collins, W. D., and Coauthors, 2004: Description of the NCAR community atmosphere model  
368 (CAM 3.0). Tech. rep., Tech. Rep. NCAR/TN-464+ STR.
- 369 Daly, C., M. Halbleib, J. I. Smith, W. P. Gibson, M. K. Doggett, G. H. Taylor, J. Curtis, and P. P.  
370 Pasteris, 2008: Physiographically sensitive mapping of climatological temperature and precip-  
371 itation across the conterminous United States. *International Journal of Climatology*, **28** (15),  
372 2031–2064.
- 373 Dee, D., and Coauthors, 2011: The ERA-Interim reanalysis: Configuration and performance of  
374 the data assimilation system. *Quarterly Journal of the Royal Meteorological Society*, **137** (656),  
375 553–597.

- 376 Fowler, H., S. Blenkinsop, and C. Tebaldi, 2007: Linking climate change modelling to impacts  
377 studies: recent advances in downscaling techniques for hydrological modelling. *International*  
378 *Journal of Climatology*, **27 (12)**, 1547–1578.
- 389 Fox-Rabinovitz, M., J. Côté, B. Dugas, M. Déqué, and J. L. McGregor, 2006: Variable resolution  
390 general circulation models: Stretched-grid model intercomparison project (SGMIP). *Journal of*  
381 *Geophysical Research: Atmospheres (1984–2012)*, **111 (D16)**.
- 382 Fox-Rabinovitz, M. S., G. L. Stenchikov, M. J. Suarez, and L. L. Takacs, 1997: A finite-  
383 difference GCM dynamical core with a variable-resolution stretched grid. *Monthly weather*  
384 *review*, **125 (11)**, 2943–2968.
- 385 Fox-Rabinovitz, M. S., L. L. Takacs, R. C. Govindaraju, and M. J. Suarez, 2001: A variable-  
386 resolution stretched-grid general circulation model: Regional climate simulation. *Monthly*  
387 *Weather Review*, **129 (3)**, 453–469.
- 388 Gallus Jr, W. A., and J. F. Bresch, 2006: Comparison of impacts of WRF dynamic core, physics  
389 package, and initial conditions on warm season rainfall forecasts. *Monthly weather review*,  
390 **134 (9)**, 2632–2641.
- 391 Hamlet, A. F., and D. P. Lettenmaier, 2005: Production of Temporally Consistent Gridded Precipi-  
392 tation and Temperature Fields for the Continental United States\*. *Journal of Hydrometeorology*,  
393 **6 (3)**, 330–336.
- 394 Hayhoe, K., and Coauthors, 2004: Emissions pathways, climate change, and impacts on Califor-  
395 nia. *Proceedings of the National Academy of Sciences of the United States of America*, **101 (34)**,  
396 12 422–12 427.

- 397 Hong, S.-Y., and J.-O. J. Lim, 2006: The WRF single-moment 6-class microphysics scheme  
398 (WSM6). *Asia-Pacific Journal of Atmospheric Sciences*, **42** (2), 129–151.
- 399 Hong, S.-Y., Y. Noh, and J. Dudhia, 2006: A new vertical diffusion package with an explicit  
400 treatment of entrainment processes. *Monthly Weather Review*, **134** (9), 2318–2341.
- 401 Hurrell, J. W., J. J. Hack, D. Shea, J. M. Caron, and J. Rosinski, 2008: A new sea surface temper-  
402 ature and sea ice boundary dataset for the Community Atmosphere Model. *Journal of Climate*,  
403 **21** (19), 5145–5153.
- 404 Hurrell, J. W., and Coauthors, 2013: The community earth system model: A framework for col-  
405 laborative research. *Bulletin of the American Meteorological Society*, **94** (9), 1339–1360.
- 406 Jankov, I., W. A. Gallus Jr, M. Segal, B. Shaw, and S. E. Koch, 2005: The impact of different WRF  
407 model physical parameterizations and their interactions on warm season MCS rainfall. *Weather*  
408 and forecasting, **20** (6), 1048–1060.
- 409 Kain, J. S., 2004: The Kain-Fritsch convective parameterization: an update. *Journal of Applied*  
410 *Meteorology*, **43** (1), 170–181.
- 411 Kanamitsu, M., and H. Kanamaru, 2007: Fifty-seven-year California Reanalysis Downscaling at  
412 10 km (CaRD10). Part I: System detail and validation with observations. *Journal of Climate*,  
413 **20** (22), 5553–5571.
- 414 Laprise, R., and Coauthors, 2008: Challenging some tenets of regional climate modelling. *Meteo-*  
415 *rology and Atmospheric Physics*, **100** (1-4), 3–22.
- 416 Leung, L. R., L. O. Mearns, F. Giorgi, and R. L. Wilby, 2003: Regional climate research: needs  
417 and opportunities. *Bulletin of the American Meteorological Society*, **84** (1), 89–95.

- 418 Leung, L. R., and Y. Qian, 2009: Atmospheric rivers induced heavy precipitation and flooding in  
419 the western US simulated by the WRF regional climate model. *Geophysical research letters*,  
420 **36** (3).
- 421 Leung, L. R., Y. Qian, X. Bian, W. M. Washington, J. Han, and J. O. Roads, 2004: Mid-century  
422 ensemble regional climate change scenarios for the western United States. *Climatic Change*,  
423 **62** (1-3), 75–113.
- 424 Lo, J. C.-F., Z.-L. Yang, and R. A. Pielke, 2008: Assessment of three dynamical climate downscal-  
425 ing methods using the Weather Research and Forecasting (WRF) model. *Journal of Geophysical*  
426 *Research: Atmospheres (1984–2012)*, **113** (D9).
- 427 Maurer, E., A. Wood, J. Adam, D. Lettenmaier, and B. Nijssen, 2002: A long-term hydrologically  
428 based dataset of land surface fluxes and states for the conterminous United States\*. *Journal of*  
429 *climate*, **15** (22), 3237–3251.
- 430 McDonald, A., 2003: Transparent boundary conditions for the shallow-water equations: testing in  
431 a nested environment. *Monthly weather review*, **131** (4), 698–705.
- 432 Mearns, L. O., and Coauthors, 2012: The North American regional climate change assessment  
433 program: overview of phase I results. *Bulletin of the American Meteorological Society*, **93** (9),  
434 1337–1362.
- 435 Mesinger, F., and K. Veljovic, 2013: Limited area NWP and regional climate modeling: a test  
436 of the relaxation vs Eta lateral boundary conditions. *Meteorology and Atmospheric Physics*,  
437 **119** (1-2), 1–16.
- 438 Mesinger, F., and Coauthors, 2006: North American regional reanalysis. *Bulletin of the American*  
439 *Meteorological Society*, **87**, 343–360.

- <sup>440</sup> Neale, R. B., and Coauthors, 2010: Description of the NCAR community atmosphere model  
<sup>441</sup> (CAM 5.0). *NCAR Tech. Note NCAR/TN-486+ STR.*
- <sup>442</sup> Pan, L.-L., S.-H. Chen, D. Cayan, M.-Y. Lin, Q. Hart, M.-H. Zhang, Y. Liu, and J. Wang, 2011:  
<sup>443</sup> Influences of climate change on California and Nevada regions revealed by a high-resolution  
<sup>444</sup> dynamical downscaling study. *Climate dynamics*, **37 (9-10)**, 2005–2020.
- <sup>445</sup> Pierce, D. W., and Coauthors, 2013: Probabilistic estimates of future changes in California temper-  
<sup>446</sup> ature and precipitation using statistical and dynamical downscaling. *Climate Dynamics*, **40 (3-**  
<sup>447</sup> **4)**, 839–856.
- <sup>448</sup> Rauscher, S. A., E. Coppola, C. Piani, and F. Giorgi, 2010: Resolution effects on regional climate  
<sup>449</sup> model simulations of seasonal precipitation over Europe. *Climate dynamics*, **35 (4)**, 685–711.
- <sup>450</sup> Rauscher, S. A., T. D. Ringler, W. C. Skamarock, and A. A. Mirin, 2013: Exploring a Global  
<sup>451</sup> Multiresolution Modeling Approach Using Aquaplanet Simulations. *Journal of Climate*, **26 (8)**,  
<sup>452</sup> 2432–2452.
- <sup>453</sup> Skamarock, W., J. Klemp, J. Dudhia, D. Gill, and D. Barker, 2005: Coauthors, 2008: A Descrip-  
<sup>454</sup> tion of the Advanced Research WRF Version 3. NCAR Technical Note. Tech. rep., NCAR/TN–  
<sup>455</sup> 475+ STR.
- <sup>456</sup> Soares, P. M., R. M. Cardoso, P. M. Miranda, J. de Medeiros, M. Belo-Pereira, and F. Espírito-  
<sup>457</sup> Santo, 2012: WRF high resolution dynamical downscaling of ERA-Interim for Portugal. *Cli-  
mate dynamics*, **39 (9-10)**, 2497–2522.
- <sup>459</sup> Staniforth, A. N., and H. L. Mitchell, 1978: A variable-resolution finite-element technique for  
<sup>460</sup> regional forecasting with the primitive equations. *Monthly Weather Review*, **106 (4)**, 439–447.

- 461 Stauffer, D. R., and N. L. Seaman, 1990: Use of four-dimensional data assimilation in a limited-  
462 area mesoscale model. Part I: Experiments with synoptic-scale data. *Monthly Weather Review*,  
463 **118** (6), 1250–1277.
- 464 Taylor, M. A., and A. Fournier, 2010: A compatible and conservative spectral element method on  
465 unstructured grids. *Journal of Computational Physics*, **229** (17), 5879–5895.
- 466 Thornton, P. E., H. Hasenauer, and M. A. White, 2000: Simultaneous estimation of daily solar ra-  
467 diation and humidity from observed temperature and precipitation: an application over complex  
468 terrain in Austria. *Agricultural and Forest Meteorology*, **104** (4), 255–271.
- 469 Thornton, P. E., and S. W. Running, 1999: An improved algorithm for estimating incident daily  
470 solar radiation from measurements of temperature, humidity, and precipitation. *Agricultural and*  
471 *Forest Meteorology*, **93** (4), 211–228.
- 472 Thornton, P. E., S. W. Running, and M. A. White, 1997: Generating surfaces of daily meteorolog-  
473 ical variables over large regions of complex terrain. *Journal of Hydrology*, **190** (3), 214–251.
- 474 Ullrich, P. A., 2014: SQuadGen: Spherical Quadrilateral Grid Generator. Accessed: 2015-02-11,  
475 <http://climate.ucdavis.edu/squadgen.php>.
- 476 Warner, T. T., R. A. Peterson, and R. E. Treadon, 1997: A tutorial on lateral boundary conditions  
477 as a basic and potentially serious limitation to regional numerical weather prediction. *Bulletin*  
478 *of the American Meteorological Society*, **78** (11), 2599–2617.
- 479 Wehner, M., Prabhat, K. Reed, D. Stone, W. D. Collins, J. Bacmeister, and A. Gettleman, 2014a:  
480 Resolution dependence of future tropical cyclone projections of CAM5.1 in the US CLIVAR  
481 Hurricane Working Group idealized configurations. *J. Climate*, doi:10.1175/JCLI-D-14-00311.  
482 1, in press.

- 483 Wehner, M. F., and Coauthors, 2014b: The effect of horizontal resolution on simulation qual-  
484 ity in the Community Atmospheric Model, CAM5.1. *J. Model. Earth. Sys.*, doi:10.1002/  
485 2013MS000276.
- 486 Zarzycki, C. M., and C. Jablonowski, 2014: A multidecadal simulation of Atlantic tropical cy-  
487 clones using a variable-resolution global atmospheric general circulation model. *Journal of Ad-*  
488 *vances in Modeling Earth Systems*, **6** (3), 805–828.
- 489 Zarzycki, C. M., C. Jablonowski, and M. A. Taylor, 2014: Using Variable-Resolution Meshes  
490 to Model Tropical Cyclones in the Community Atmosphere Model. *Monthly Weather Review*,  
491 **142** (3), 1221–1239.
- 492 Zarzycki, C. M., C. Jablonowski, D. R. Thatcher, and M. A. Taylor, 2015a: Assessing the model  
493 climatology of a multidecadal variable-resolution global atmospheric general circulation model  
494 simulation. *Journal of Climate*, in review.
- 495 Zarzycki, C. M., C. Jablonowski, D. R. Thatcher, and M. A. Taylor, 2015b: Effects of local-  
496 ized grid refinement on the general circulation and climatology in the Community Atmosphere  
497 Model. *Journal of Climate*, (2015).

498 **LIST OF TABLES**

499	<b>Table 1.</b> Reanalysis or statistically downscaled observational datasets . . . . .	26
500	<b>Table 2.</b> RMSE and Bias for JJA temperature (California) . . . . .	27
501	<b>Table 3.</b> RMSE and Bias for DJF temperature (California) . . . . .	28
502	<b>Table 4.</b> RMSE and Bias for Precipitation (California) . . . . .	29
503	<b>Table 5.</b> Seasonal Average Precipitation for five sub-divisions of California . . . . .	30

TABLE 1. Reanalysis or statistically downscaled observational datasets

<b>Data source</b>	<b>Variables used</b>	<b>Spatial resolution</b>	<b>Temporal resolution</b>
<b>UW</b>	Pr, $T_{min}$ , $T_{max}$	0.125°	daily
<b>PRISM</b>	Pr, $T_{min}$ , $T_{max}$ , $T_{avg}$	4km	monthly/daily
<b>DAYMET</b>	Pr, $T_{min}$ , $T_{max}$	1km	daily
<b>NCEP CPC</b>	Pr	0.125°	daily
<b>NARR</b>	Pr, $T_s$	32km	daily

TABLE 2. RMSE and Bias for JJA temperature (California)

RMSE	UW		PRISM			DAYMET	
	T <sub>max</sub>	T <sub>min</sub>	T <sub>max</sub>	T <sub>min</sub>	T <sub>avg</sub>	T <sub>max</sub>	T <sub>min</sub>
<b>varres-CESM 0.25d</b>	2.324	3.752	2.932	3.136	2.614	2.810	3.938
<b>varres-CESM 0.125d</b>	1.903	3.639	2.452	2.961	2.195	2.477	3.707
<b>WRF 27km</b>	2.311	2.741	2.924	2.252	2.161	2.511	2.993
<b>WRF 9km</b>	3.319	2.943	3.470	1.847	1.752	3.203	2.945

BIAS	UW		PRISM			DAYMET	
	T <sub>max</sub>	T <sub>min</sub>	T <sub>max</sub>	T <sub>min</sub>	T <sub>avg</sub>	T <sub>max</sub>	T <sub>min</sub>
<b>varres-CESM 0.25d</b>	0.982	2.913	0.631	1.756	0.847	1.177	2.882
<b>varres-CESM 0.125d</b>	0.651	2.857	0.233	1.687	0.607	0.824	2.752
<b>WRF 27km</b>	-0.574	0.820	-0.925	-0.337	-0.747	-0.383	0.790
<b>WRF 9km</b>	-2.274	1.868	-2.693	0.698	-1.118	-2.101	1.762

TABLE 3. RMSE and Bias for DJF temperature (California)

	RMSE		UW			PRISM			DAYMET	
	T <sub>max</sub>	T <sub>min</sub>	T <sub>max</sub>	T <sub>min</sub>	T <sub>avg</sub>	T <sub>max</sub>	T <sub>min</sub>	T <sub>max</sub>	T <sub>min</sub>	
<b>varres-CESM 0.25d</b>	1.605	3.035	2.098	2.393	1.753	2.109	3.170			
<b>varres-CESM 0.125d</b>	1.903	1.226	2.804	1.772	1.501	1.871	2.884			
<b>WRF 27km</b>	1.710	2.506	2.240	1.729	1.721	2.105	2.691			
<b>WRF 9km</b>	2.517	2.769	2.732	1.764	1.420	2.581	2.752			

BIAS	UW		PRISM			DAYMET	
	T <sub>max</sub>	T <sub>min</sub>	T <sub>max</sub>	T <sub>min</sub>	T <sub>avg</sub>	T <sub>max</sub>	T <sub>min</sub>
<b>varres-CESM 0.25d</b>	-0.082	2.385	-0.353	1.296	-0.269	-0.037	2.256
<b>varres-CESM 0.125d</b>	-0.241	2.229	-0.559	1.130	-0.438	-0.224	2.031
<b>WRF 27km</b>	-0.379	1.409	-0.649	0.321	-0.729	-0.336	1.282
<b>WRF 9km</b>	-1.805	2.166	-2.123	1.067	-0.891	-1.786	1.967

TABLE 4. RMSE and Bias for Precipitation (California)

<b>Annual</b>	<b>CPC</b>		<b>UW</b>		<b>PRISM</b>		<b>DAYMET</b>	
	RMSE	Bias	RMSE	Bias	RMSE	Bias	RMSE	Bias
<b>varres-CESM 0.25d</b>	0.590	0.370	0.604	0.265	0.726	0.171	0.560	0.169
<b>varres-CESM 0.125d</b>	0.481	0.220	0.534	0.126	0.634	0.050	0.510	0.043
<b>WRF 27km</b>	0.424	-0.210	0.586	-0.315	0.777	-0.409	0.650	-0.411
<b>WRF 9km</b>	2.204	1.462	2.026	1.368	1.858	1.292	1.986	1.286

<b>DJF</b>	<b>CPC</b>		<b>UW</b>		<b>PRISM</b>		<b>DAYMET</b>	
	RMSE	Bias	RMSE	Bias	RMSE	Bias	RMSE	Bias
<b>varres-CESM 0.25d</b>	1.409	0.883	1.401	0.558	1.636	0.465	1.310	0.404
<b>varres-CESM 0.125d</b>	1.236	0.666	1.273	0.362	1.436	0.307	1.210	0.234
<b>WRF 27km</b>	0.918	-0.396	1.331	-0.721	1.588	-0.815	1.389	-0.876
<b>WRF 9km</b>	4.244	2.562	3.801	2.257	3.538	2.203	3.782	2.132

TABLE 5. Seasonal Average Precipitation for five sub-divisions of California

	SON					DJF					MAM					JJA				
	CV	Mt	NC	SC	Dt	CV	Mt	NC	SC	Dt	CV	Mt	NC	SC	Dt	CV	Mt	NC	SC	Dt
<b>UW</b>	1.14	1.68	1.92	0.59	0.31	3.62	4.31	6.19	2.75	0.89	1.72	2.22	2.64	1.16	0.38	0.13	0.41	0.18	0.07	0.22
<b>PRISM</b>	1.21	1.82	2.17	0.64	0.31	3.49	4.50	6.39	2.93	0.89	1.75	2.38	2.84	1.25	0.39	0.14	0.46	0.22	0.05	0.25
<b>CESM 0.25d</b>	1.89	1.90	2.20	0.57	0.42	5.35	4.62	5.87	2.87	1.27	2.35	2.35	2.56	0.83	0.48	0.10	0.47	0.13	0.07	0.20
<b>CESM 0.125d</b>	1.22	1.45	1.72	0.42	0.40	4.95	4.46	5.82	2.70	1.09	2.32	2.46	2.51	1.09	0.48	0.10	0.50	0.13	0.06	0.22
<b>WRF 27km</b>	0.87	1.33	1.30	0.46	0.20	3.05	3.86	4.18	1.97	0.47	1.44	2.12	1.84	0.94	0.20	0.10	0.57	0.21	0.10	0.08
<b>WRF 9km</b>	2.13	3.69	3.35	1.20	0.97	5.74	8.26	8.84	4.10	1.08	3.05	4.38	4.18	1.71	0.49	0.32	1.78	0.43	0.24	0.80

## 504 LIST OF FIGURES

505	<b>Fig. 1.</b> Domains of WRF simulations (Bottom left) and five climate divisions in California (Upper right). . . . .	32
506		
507	<b>Fig. 2.</b> The domains of varres-CESM simulations . . . . .	33
508		
509	<b>Fig. 3.</b> Topography fields in meters (m) for (top left to bottom right) varres-CESM 0.25deg, varres-CESM 0.125deg, uniform CESM 0.25deg, WRF 27km, WRF 9km and ERA-Interim ~80km. . . . .	34
510		
511	<b>Fig. 4.</b> JJA average daily Tmax from models and reference datasets, and differences between them (unit: C). (Daymet is similar to PRISM, so not showed in difference plot) . . . . .	35
512		
513	<b>Fig. 5.</b> As Figure 4, but for summer Tmin. (Daymet is similar to UW, so not showed in difference plot) . . . . .	36
514		
515	<b>Fig. 6.</b> As Figure 4, but for Tavg in JJA and DJF. . . . .	37
516		
517	<b>Fig. 7.</b> As Figure 4, but for winter Tmax. . . . .	38
518		
519	<b>Fig. 8.</b> As Figure 4, but for winter Tmin. . . . .	39
520		
521	<b>Fig. 9.</b> Seasonal cycle of monthly-average Tavg for each subzone ( $^{\circ}$ C) Errorbars represent standard deviation ( $\sigma$ ) values. . . . .	40
522		
523	<b>Fig. 10.</b> Frequency distribution of summer Tmax ( $^{\circ}$ C). . . . .	41
524		
525	<b>Fig. 11.</b> Annual average daily total precipitation from models and reference datasets (mm/d). . . . .	42
526		
527	<b>Fig. 12.</b> As Figure 11, but for winter (DJF) total precipitation (mm/d). . . . .	43
528		
529	<b>Fig. 13.</b> As Figure 9, but for monthly-average total precipitation (mm/d). . . . .	44
530		
531	<b>Fig. 14.</b> Frequency distribution of winter Pr constructed from 26 years daily data (mm/d) (note that the vertical scale is logarithmic). . . . .	45
532		
533	<b>Fig. 15.</b> Taylor diagram of annual climatology for the region of CA, using PRISM dataset as reference . . . . .	46
534		
535	<b>Fig. 16.</b> Climatology simulation comparison between varres-CESM 0.25 deg and uniform CESM-FV 0.25 deg . . . . .	47
536		

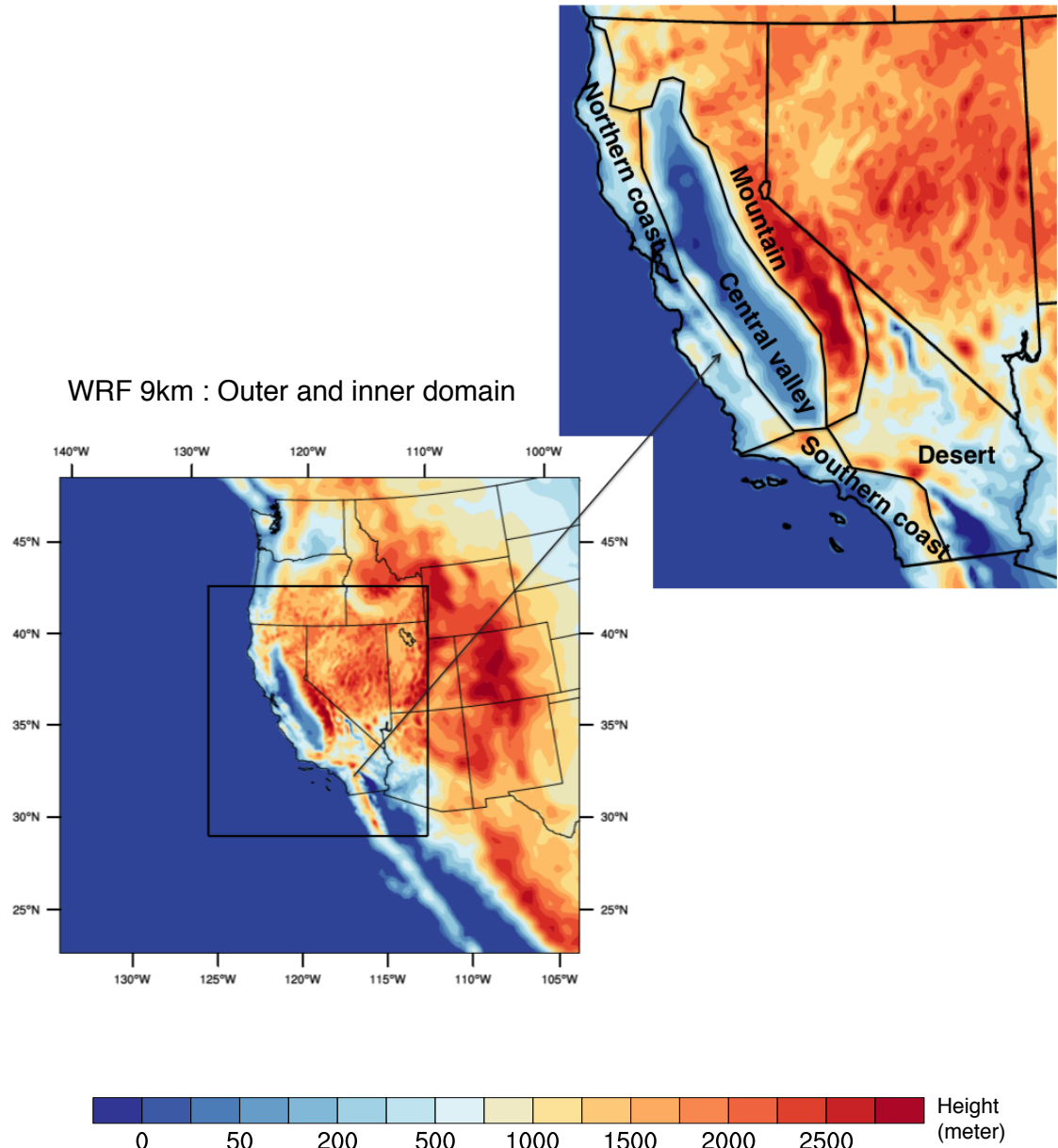


FIG. 1. Domains of WRF simulations (Bottom left) and five climate divisions in California (Upper right).

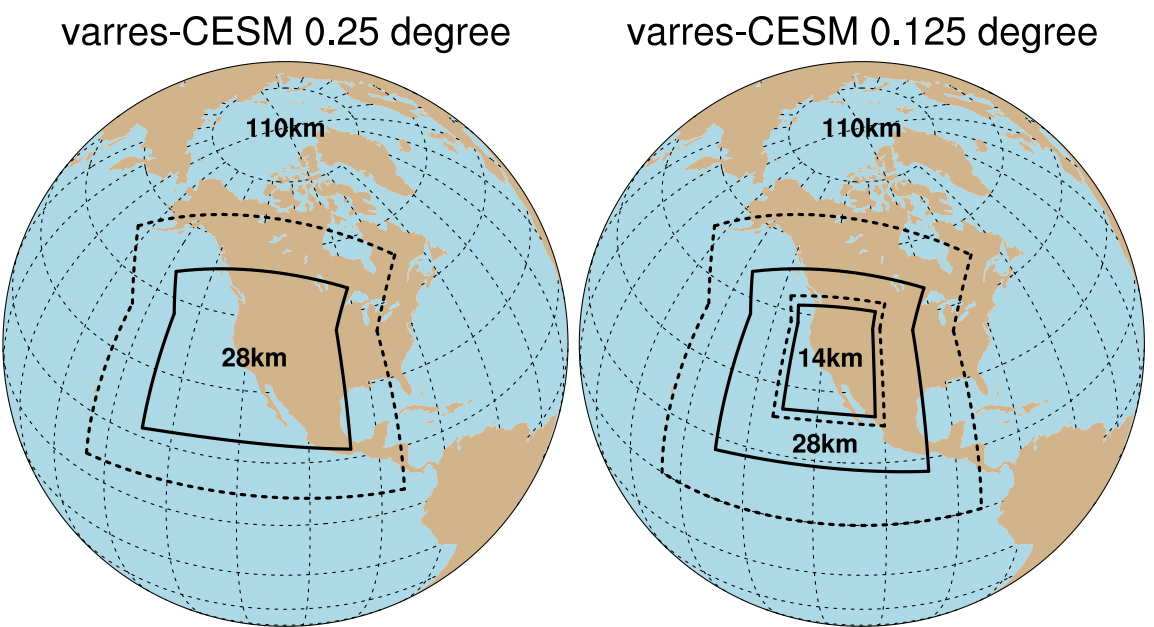
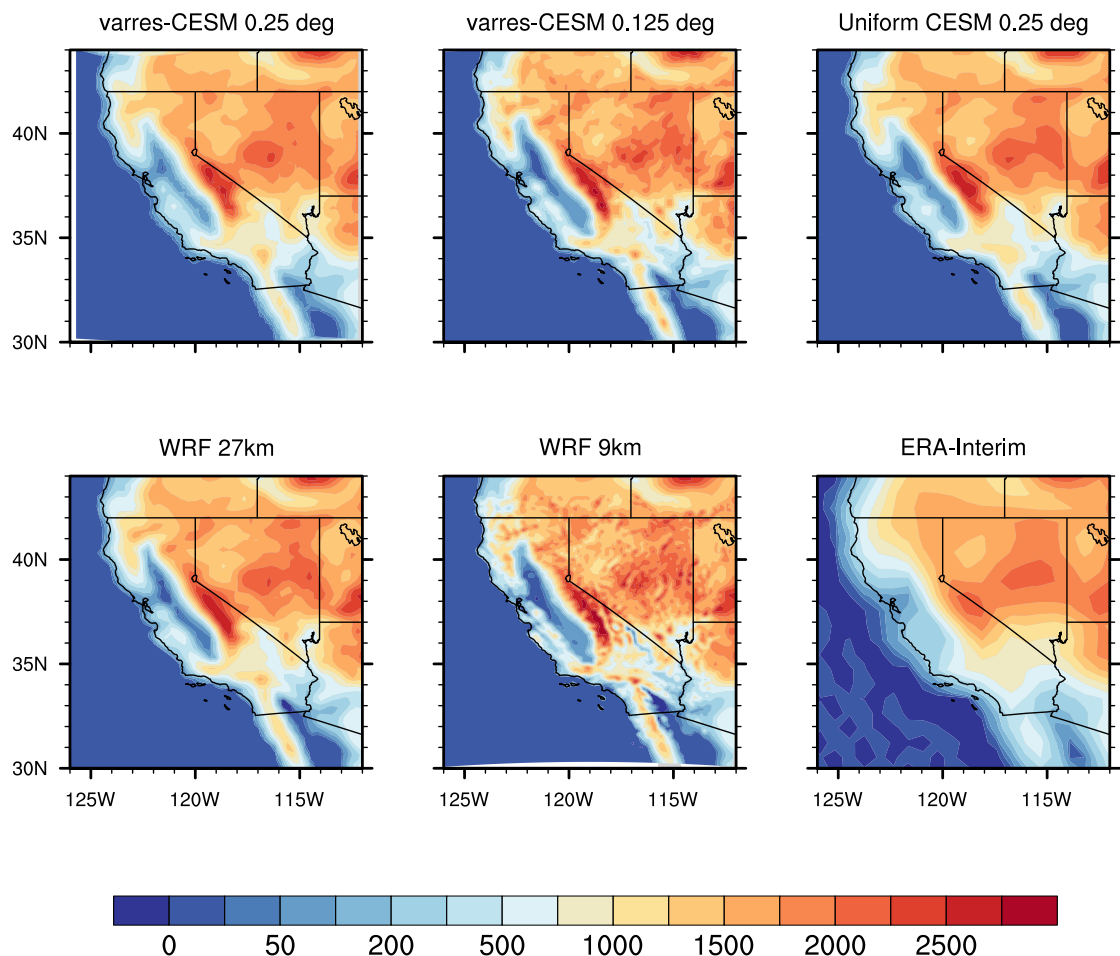
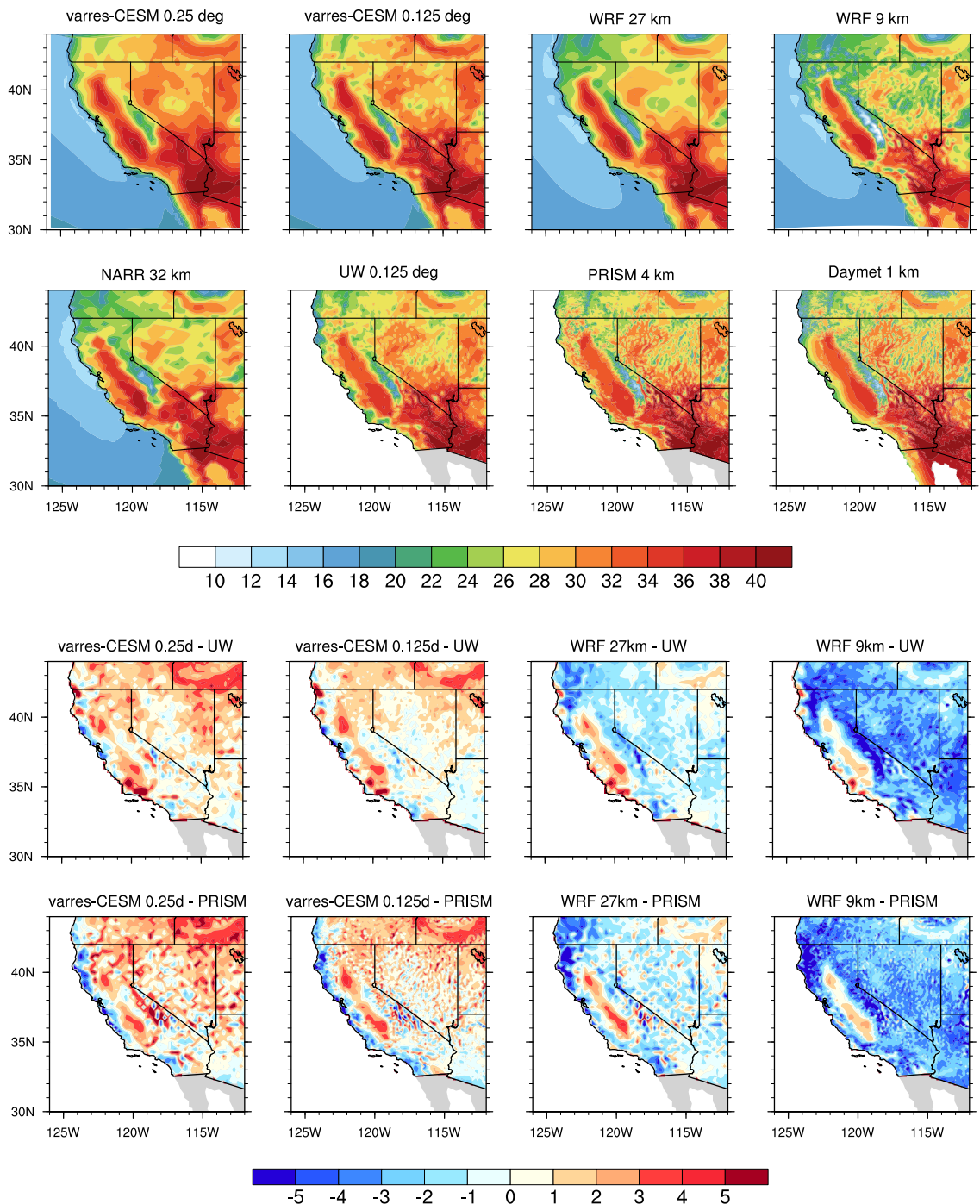


FIG. 2. The domains of varres-CESM simulations



530 FIG. 3. Topography fields in meters (m) for (top left to bottom right) varres-CESM 0.25deg, varres-CESM  
 531 0.125deg, uniform CESM 0.25deg, WRF 27km, WRF 9km and ERA-Interim ~80km.



532 FIG. 4. JJA average daily Tmax from models and reference datasets, and differences between them (unit: C).  
 533 (Daymet is similar to PRISM, so not showed in difference plot)

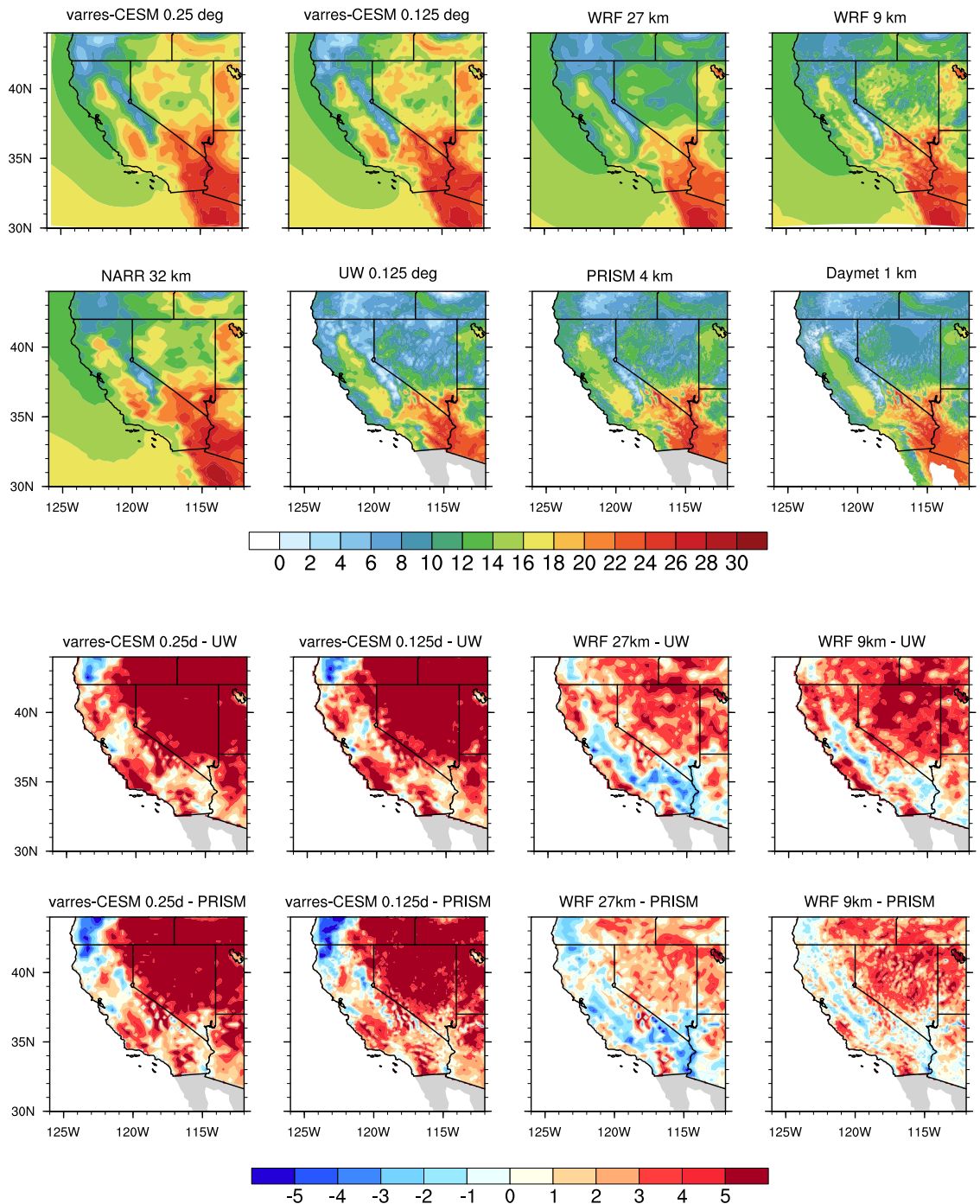


FIG. 5. As Figure 4, but for summer Tmin. (Daymet is similar to UW, so not showed in difference plot)

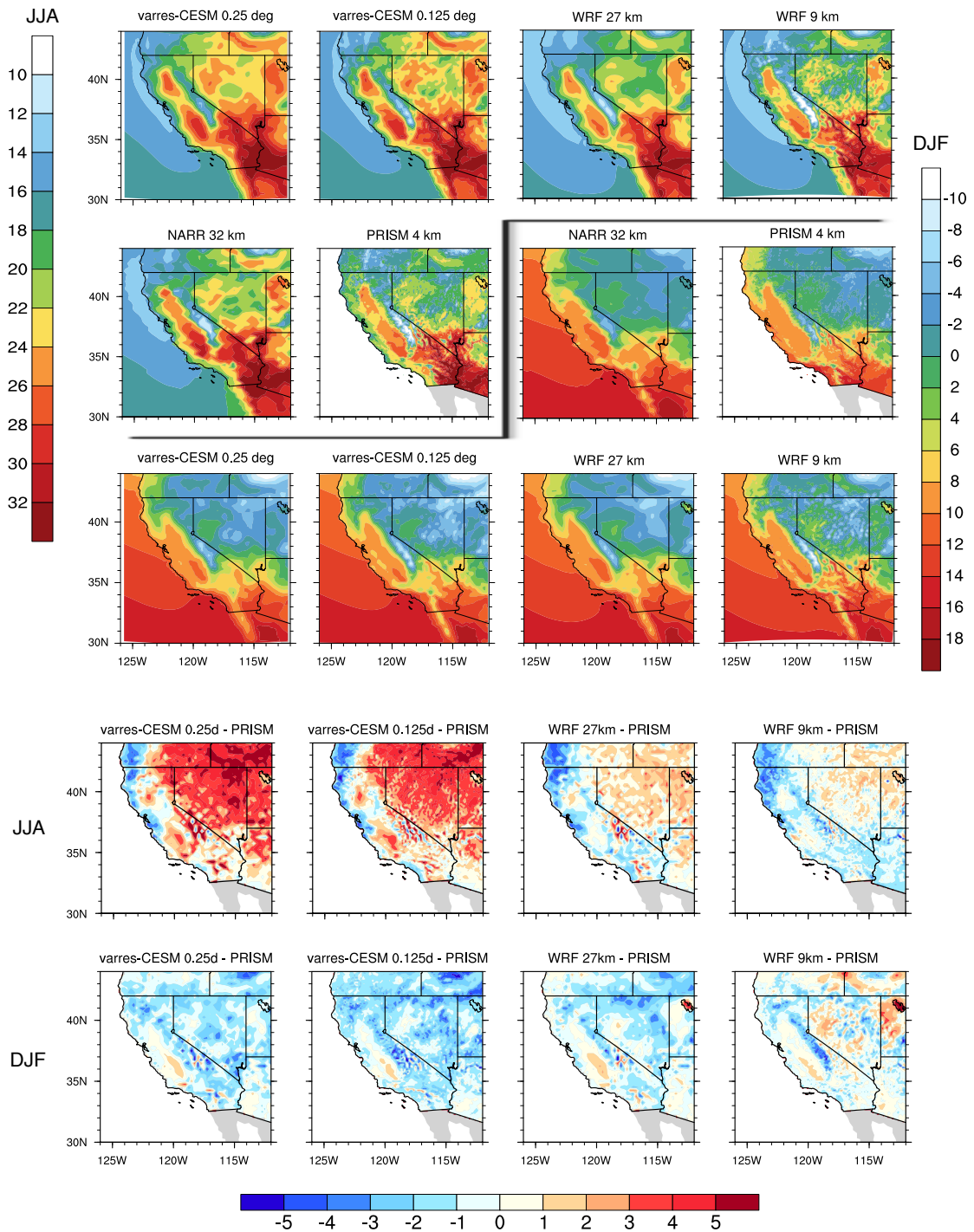


FIG. 6. As Figure 4, but for Tavg in JJA and DJF.

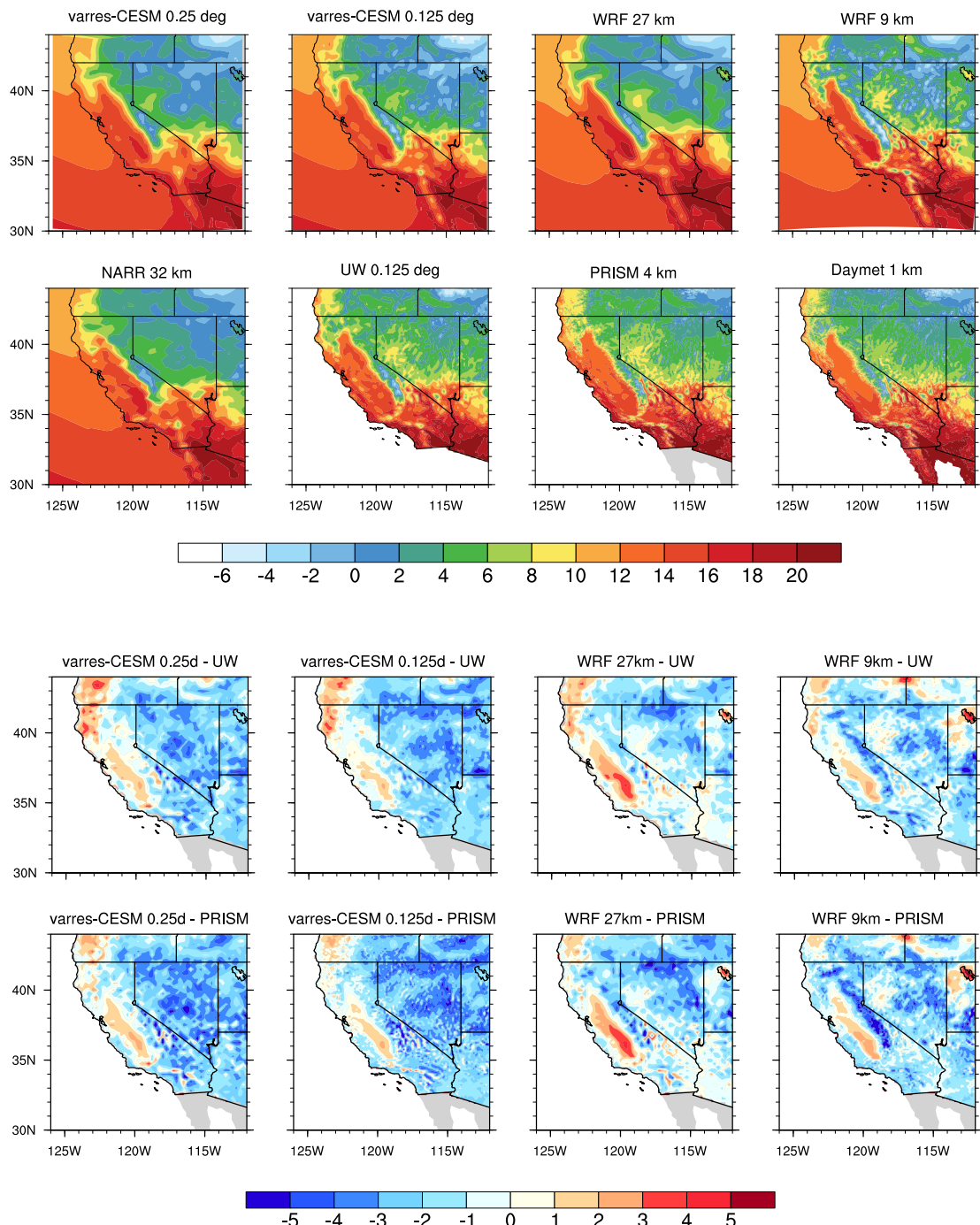


FIG. 7. As Figure 4, but for winter Tmax.

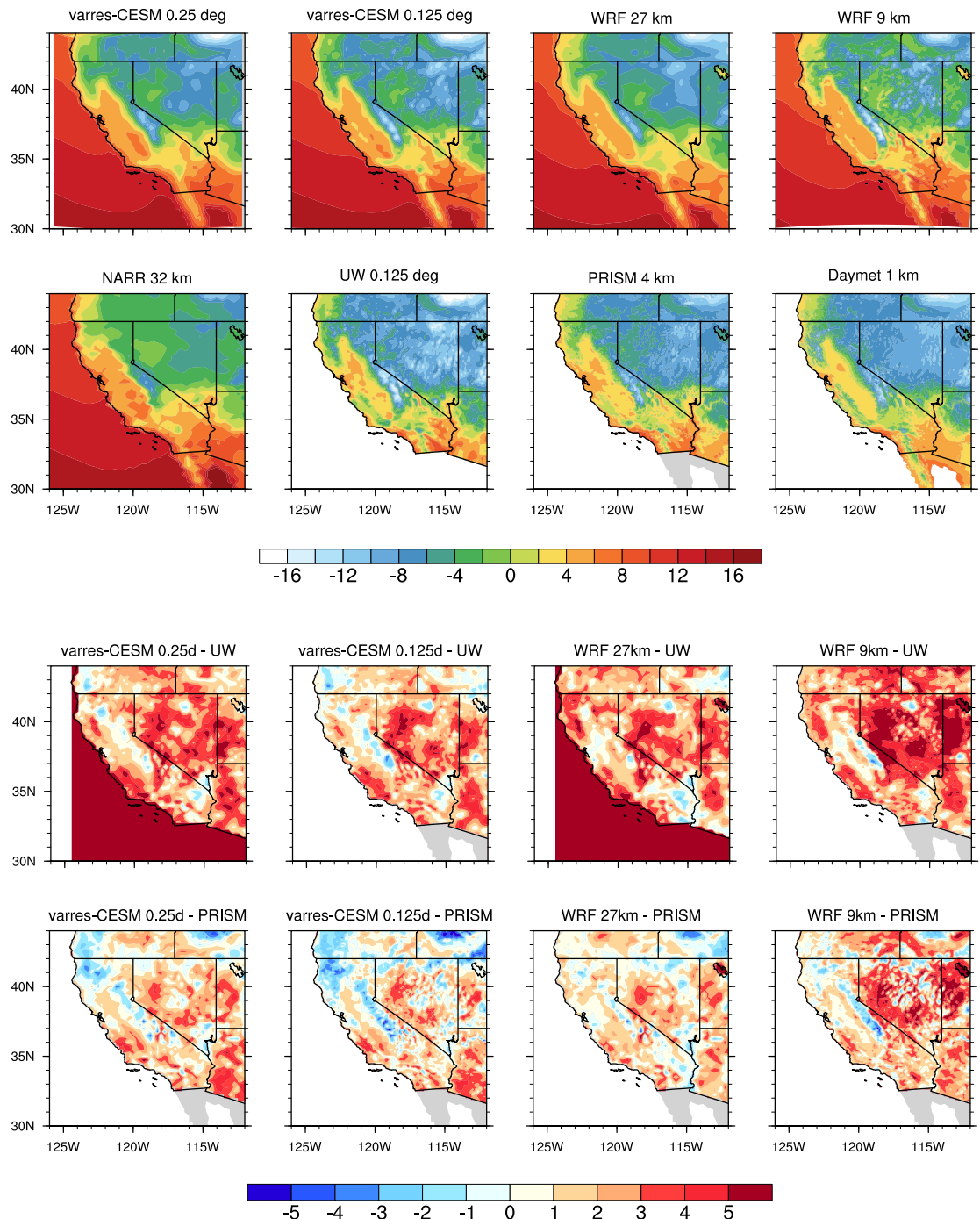
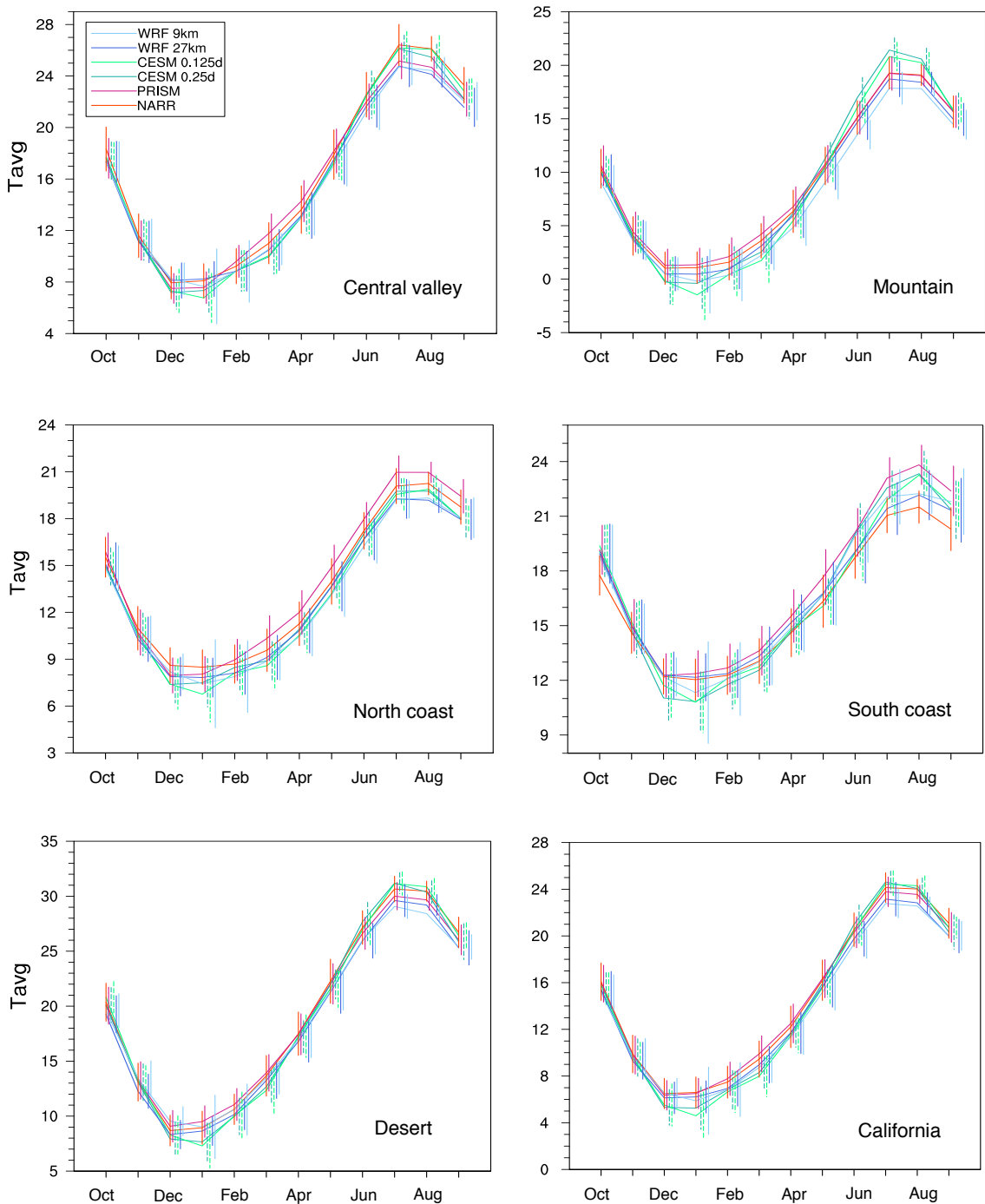


FIG. 8. As Figure 4, but for winter Tmin.



534 FIG. 9. Seasonal cycle of monthly-average Tavg for each subzone ( $^{\circ}\text{C}$ ) Errorbars represent standard deviation  
 535 ( $\sigma$ ) values.

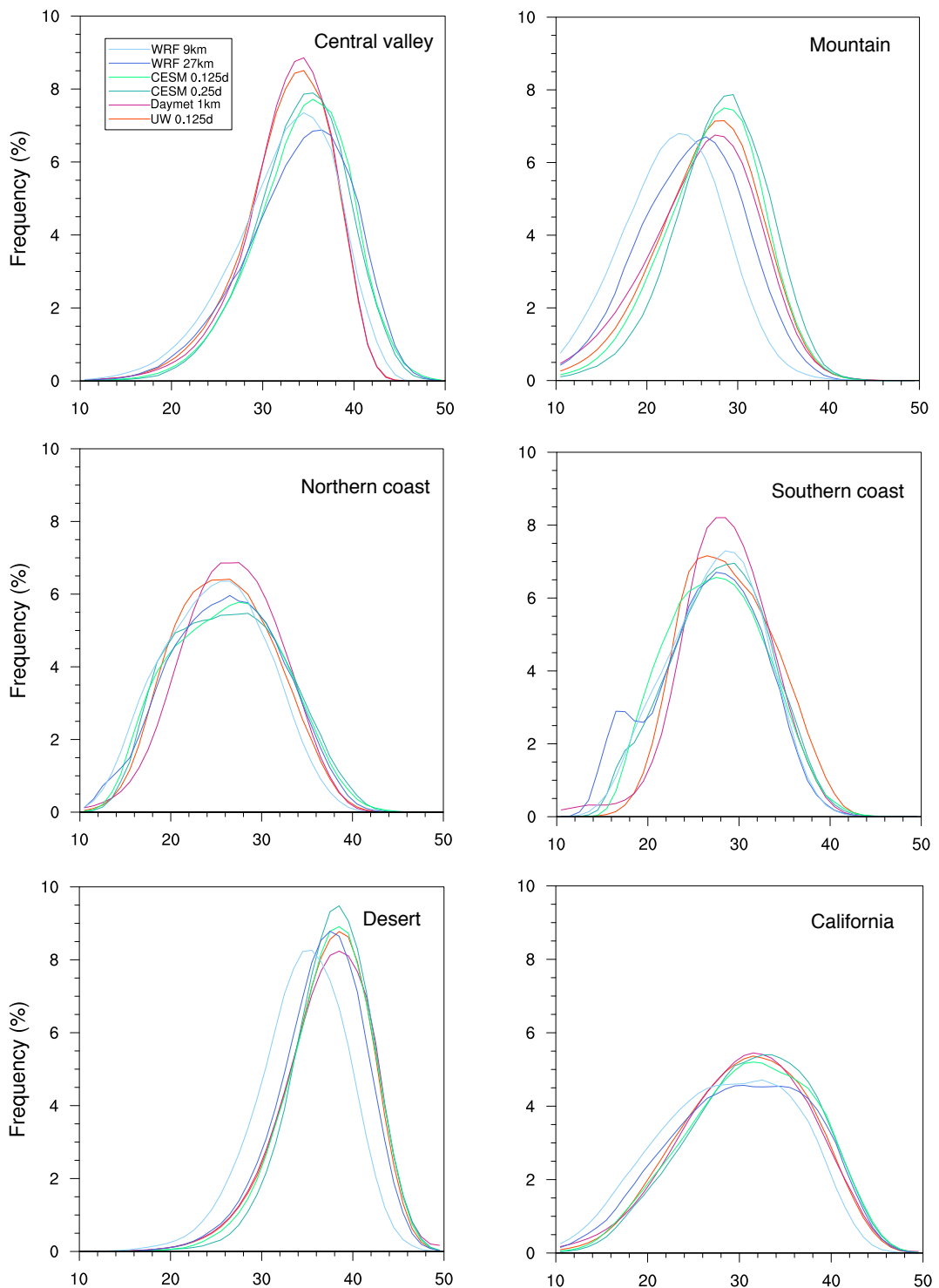


FIG. 10. Frequency distribution of summer Tmax ( $^{\circ}\text{C}$ ).

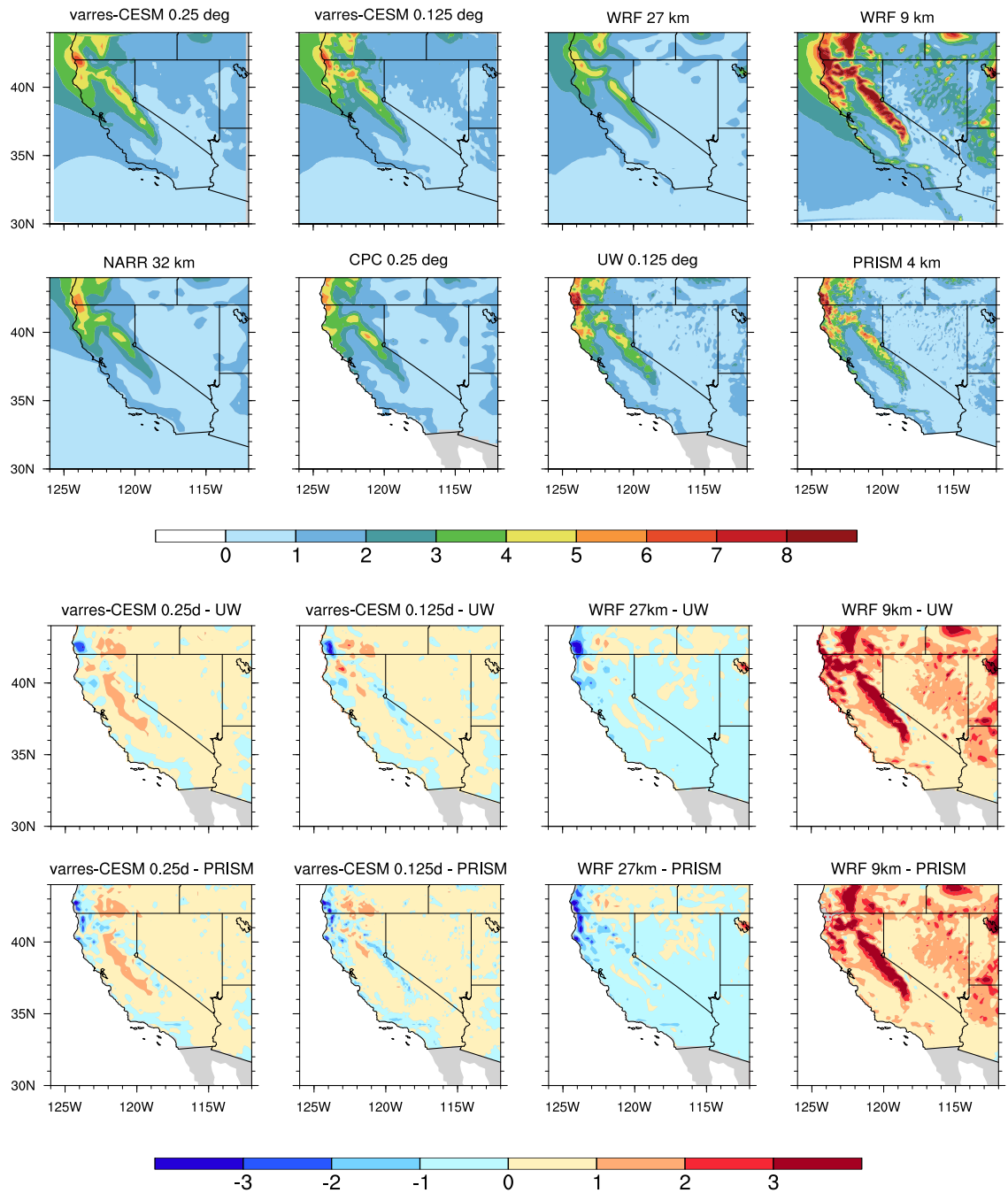


FIG. 11. Annual average daily total precipitation from models and reference datasets (mm/d).

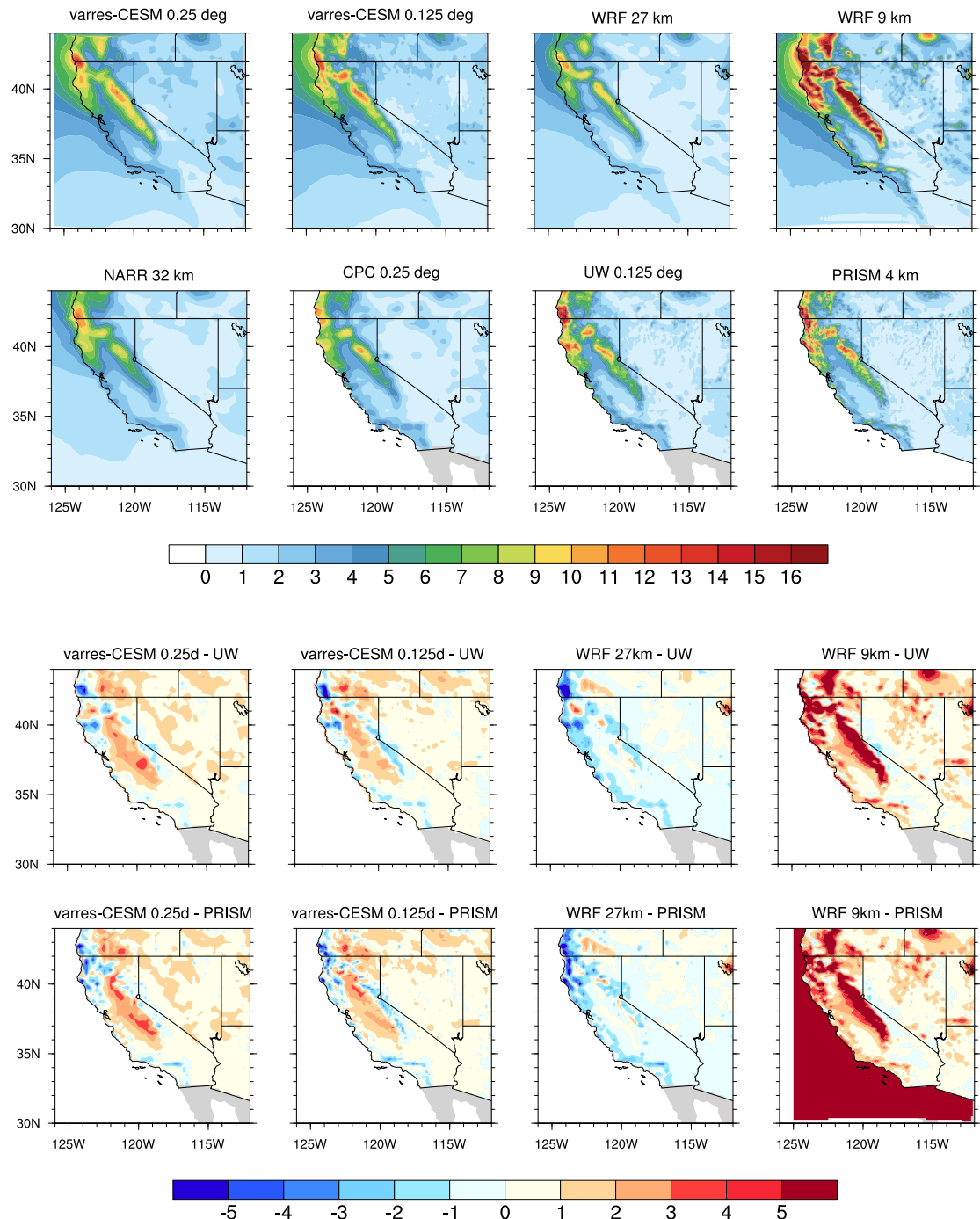


FIG. 12. As Figure 11, but for winter (DJF) total precipitation (mm/d).

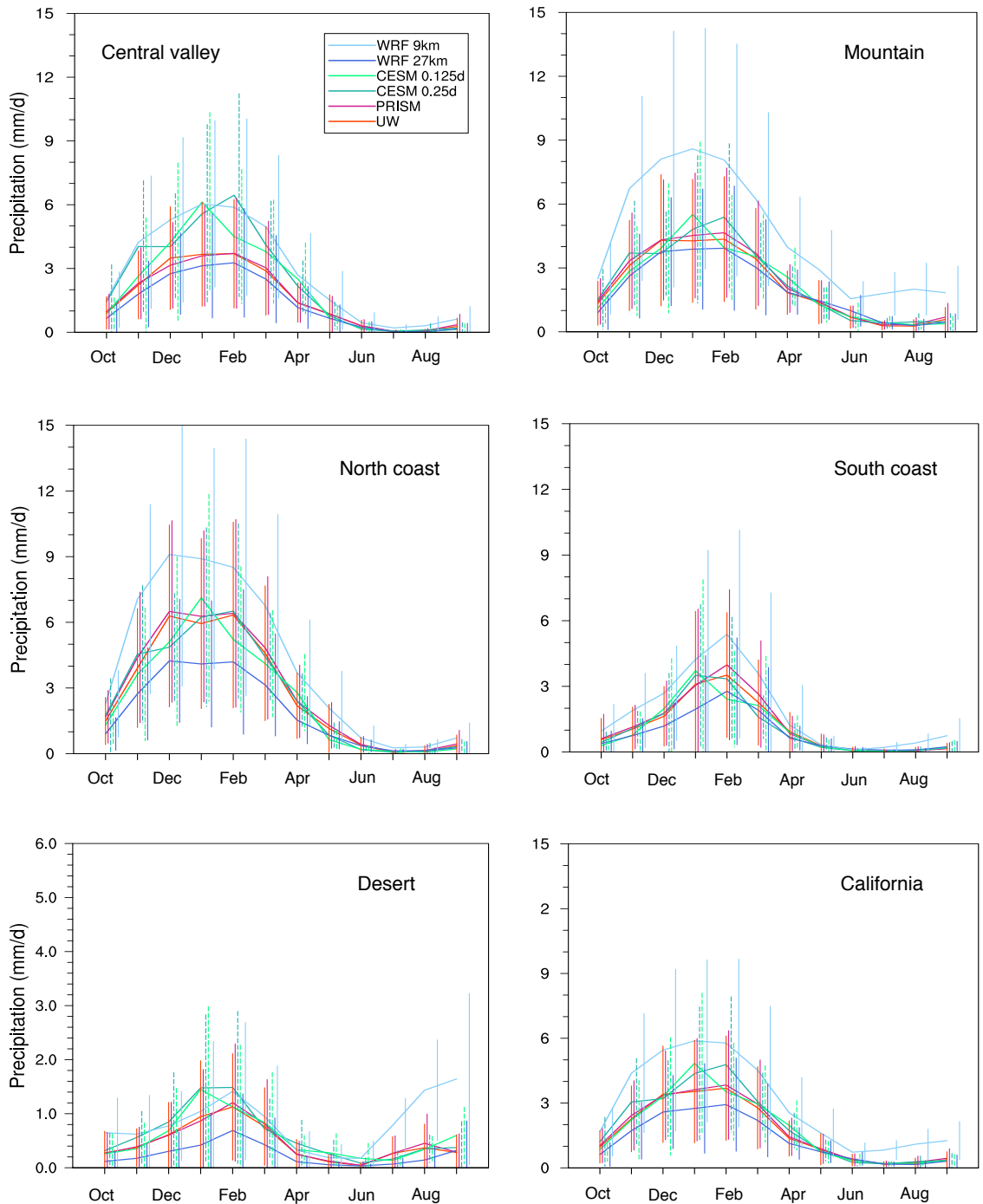
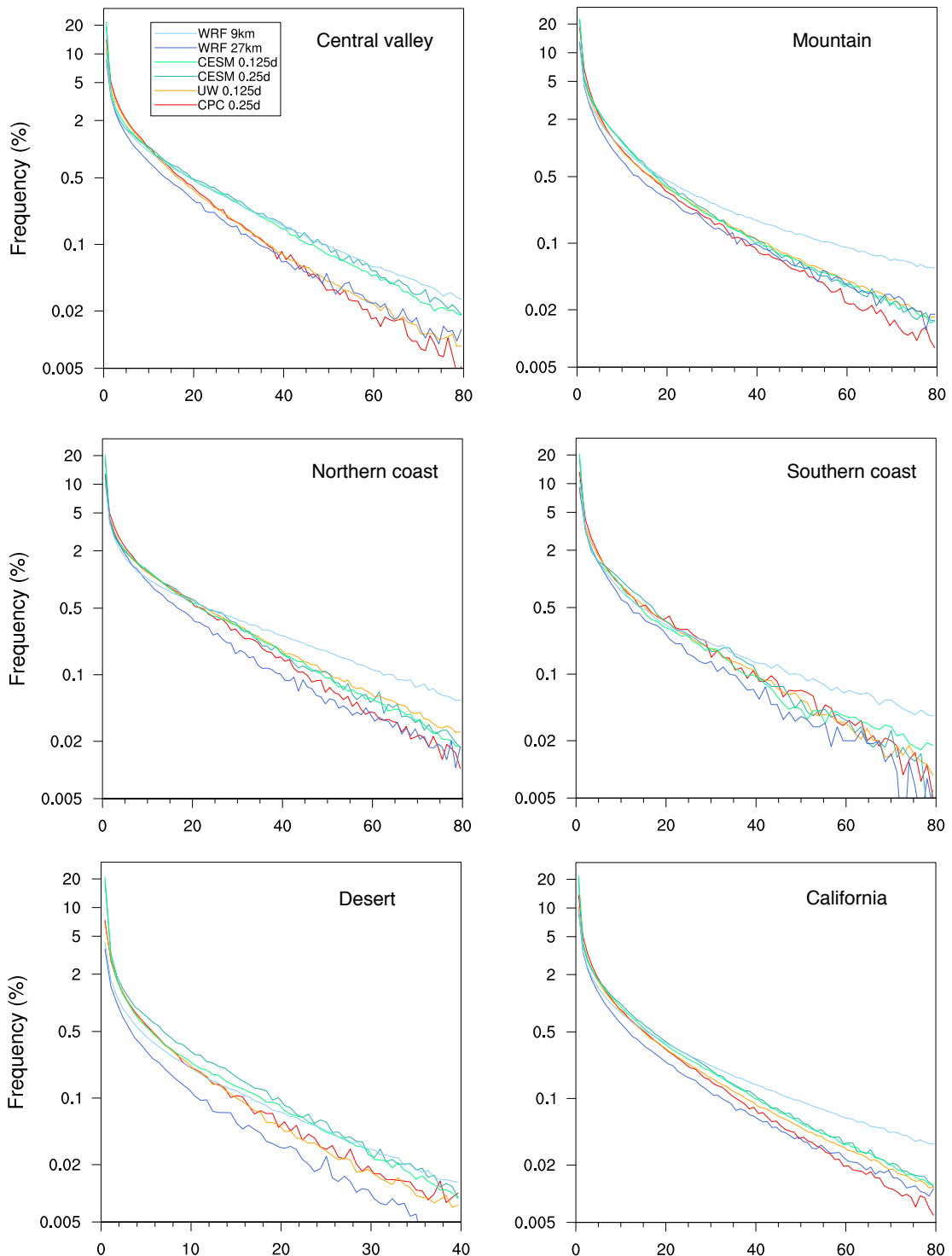


FIG. 13. As Figure 9, but for monthly-average total precipitation (mm/d).



536 FIG. 14. Frequency distribution of winter Pr constructed from 26 years daily data (mm/d) (note that the  
 537 vertical scale is logarithmic).

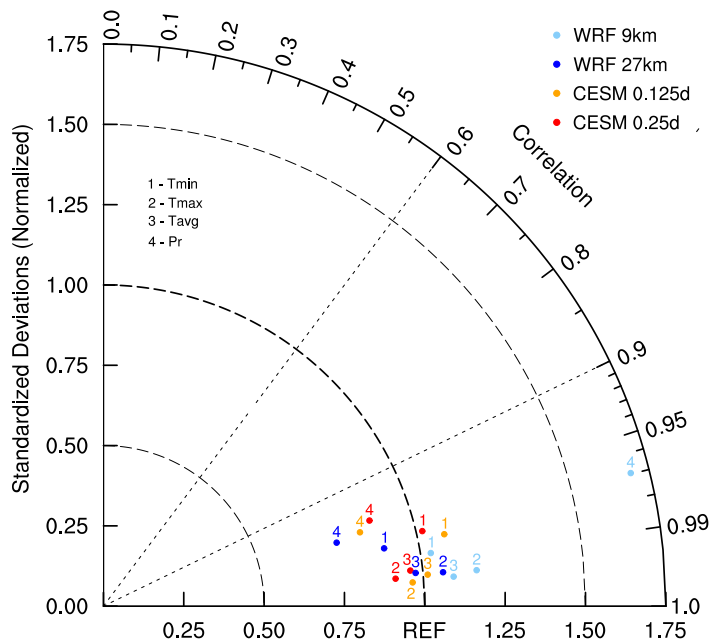


FIG. 15. Taylor diagram of annual climatology for the region of CA, using PRISM dataset as reference

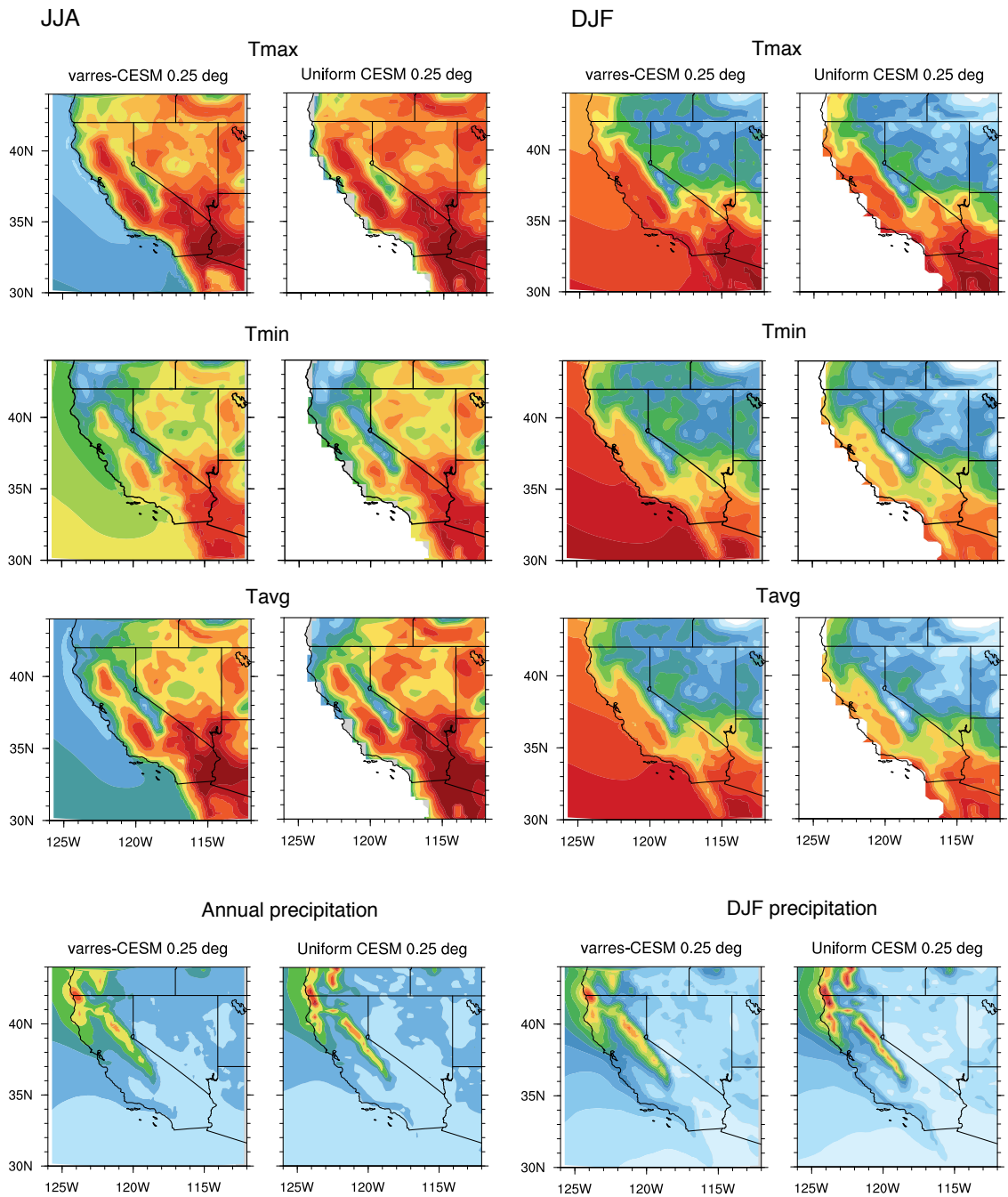


FIG. 16. Climatology simulation comparison between varres-CESM 0.25 deg and uniform CESM-FV 0.25 deg